UNIVERSITY OF UTAH
DEPARTMENT OF PHYSICS
SALT LAKE CITY, UTAH 84112

TECHNICAL REPORT

FOR PERIOD ENDING JULY 31, 1972

to

ADVANCED RESEARCH PROJECT AGENCY

Principal Investigators

John W. DeFord (Phone 801 581-6971)
Associate Professor of Physics

Owen W. Johnson (Phone 801 581-7166)
Associate Professor of Physics
and
Adjunct Associate Professor of Materials Science and Engineering

Franz Rosenberger (Phone 801 581-8373)
Assistant Research Professor
and
Director of Crystal Growth Laboratory

Title

ELECTRONIC AND RADIATION DAMAGE PROPERTIES OF RUTILE

Period: 1 year

Date: 15 June 1971 to
31 July 1972

Amount: $111,000

Grant No. DAHC 15-71-G9-0008

Contractor: Defense Supply Service - Washington

Project Monitor: Dr. O. C. Trulson
Deputy Director for Materials Sciences
Advanced Research Projects Agency
Washington, D. C. 20301

Sponsored By
Advanced Research Projects Agency
ARPA Order No. 1610

This report covers the period from December 1, 1971 to July 31, 1972. During this period work was concentrated in the following areas.

A. Crystal Growth
B. Hydrogen Kinetics - Theoretical
C. Hydrogen Kinetics - Experimental
D. Devices
E. Review Paper
F. Far IR Spectroscopy
G. Magnetic Resonance Study of Defect States
H. Free Carrier Optical Absorption
I. Hydrogen Diffusion
J. Electron Trapping States

Each area will be discussed separately in what follows.

A. Crystal Growth

The present status of the rutile crystal growth project is extremely encouraging. We have now achieved highly reproducible growth rates of the order of 1 mm/day. The resulting crystals appear to be of very high quality and it now appears almost certain that this growth technique will indeed live up to all of our expectations and enable us to produce crystals of much higher perfection and purity than have ever been achieved before. A rather surprising number of problems, some of a very fundamental nature, had to be overcome to reach our present position. Details on some of the

more significant problems are given below:

1. Transport Mechanism

Very little information had been available concerning the thermal stability of the transport agent $TeCl_4$, which is obviously of great importance in understanding the transport mechanism: Firstly, the chemical kinetics depend on the availability of $TeCl_4$ in the growth ampoule. Secondly, a temperature-dependent, reversible dissociation such as

$$TeCl_4 \rightleftarrows TeCl_2 + Cl_2 \quad , \qquad (1)$$

could establish density gradients in addition to the gradients resulting from the temperature profile, and thus enhance the driving force for convection and material transfer. It was felt that by an appropriate choice of the growth temperatures (within the limits imposed by chemical and interface kinetics considerations), this additional transport mechanism could be optimized, if a more quantitative understanding of (1) could be achieved. Thus, calculations of the kinetics of this reaction were performed, based on available thermo-chemical data. These showed that thermal dissociation according to (1) indeed occurs, a fact only suspected hitherto. The calculation was checked by measurements of the thermal dissociation. High purity $TeCl_4$, synthesized in situ as described below, was heated in a quartz bourdon gauge and the resulting pressure determined over the temperature range of interest. The experimental results fit the theoretical values very well, taking into account the limited precision of the available heats of formation that had to be used in the calculations.

This effort has given us major insight into the complex transport mechanism. Our work has verified that the transport reaction originally

assumed,

$$TeCl_4 + TiO_2 \leftrightarrow TeO_2 + TiCl_4 \ ,$$

is indeed responsible for the TiO_2 transport. However, the calculations above show that, at the growth temperatures, the $TeCl_4$ is more than 90% dissociated according to Eq. (1). It is interesting that the loss of transport agent, due to thermal dissociation, is more than offset by the enhancement of convection due to the same reaction. This clearly demonstrates the complexity of the system we are dealing with and amply justifies our contention that a thorough, detailed understanding is absolutely essential to success in dealing with materials like TiO_2.

Various transport phenomena which we had observed earlier and were unable to explain with mere thermally induced density gradients, are qualitatively understood now. Quantitative studies of the relative weight of thermally and concentration induced convection are planned. Furthermore, with little more effort, we will be able to contribute thermodynamical information about the $TeCl_4$ system with substantially higher accuracy than are now available. Since $TeCl_4$ is quite frequently employed in the growth of oxide crystals, this information is of general importance.

2. Purity of Transport Agent

A major experimental difficulty resulted from the extreme hygroscopicity of $TeCl_4$. This uncertainty has been eliminated by synthesizing the tellurium tetrachloride in situ from high purity tellurium and high vacuum distilled chlorine. This refinement has dramatically improved the reproducibility of the transport rates.

3. Profile Inside Growth Ampoule

Further measurements of the temperature distribution inside the

growth ampoules as well as in simulated open geometries led us to a major breakthrough in devising an appropriate heating geometry. In the previously used arrangement, besides growth onto the seed, heavy deposition of TiO_2 occurred also on the wall of the growth ampoule over a zone of several centimeters. This created several problems: The growth rate was reduced by reduction of the degree of supersaturation at the seed. The ultimate size of the grown crystal was limited. Equally importantly for present purposes, the deposits on the ampoule wall obscured visual monitoring of the seed growth. A novel ampoule geometry has been developed, in which the seed is cooled by radiation to somewhat lower temperatures than the quartz wall. The technique consists essentially of weakly coupling the seed crystal to a low temperature bath (room temperature), by means of light pipe. The technique relies on the fact that the thermal emissivity of the TiO_2 is much higher than that of quartz. Thus, we are able to produce the seemingly paradoxical situation in which a seed crystal, completely enclosed in the quartz ampoule, is maintained at a temperature below that of the ampoule. This, of course, is the absolute optimum in growth conditions. Consequently, growth onto the ampoule wall is completely excluded, and all the transported material is deposited on the seed. This enables us to substantially reduce the seed-to-source temperature difference and hence, the temperature oscillations reported earlier can be avoided, even in a vertical arrangement.

Two papers on our crystal growth efforts were accepted for presentation at the Second National Meeting of the American Association for Crystal Growth in August at Princeton. The abstracts are enclosed.

GROWTH OF TiO_2 (RUTILE) BY CHEMICAL VAPOR TRANSPORT[†]

F. Rosenberger and M. C. DeLong

Physics Department, University of Utah
Salt Lake City, Utah 84112

Rutile single crystals of typically 2 cm diameter and 2 mm thickness were grown homoepitaxially in closed quartz ampoules employing the overall reaction.

$$TiO_2 + TeCl_4 \rightleftarrows TeO_2 + TiCl_4 \quad . \qquad (1)$$

Thermochemical calculations showing that $TeCl_4$ dissociates according to

$$TeCl_4 \rightleftarrows TeCl_2 + Cl_2 \qquad (2)$$

were confirmed by pressure-temperature measurements. The role of (2) in the transport mechanism is discussed.* Calculations for Cl_2, $TeCl_2$ and $TeCl_4$:Cl_2 mixtures and corresponding transport experiments give strong evidence that $TeCl_4$ is the actual transport agent.

The growth and etching form of rutile obtained in (1) was found to consist of {111} faces -- in disagreement with experimental and theoretical results hitherto reported.

Preparational procedures are described and details on the growth process which was performed in a novel heating-cooling arrangement are given.

[†]Work sponsored by the Advanced Research Projects Agency on Grant No. DAHC-15-71-G8.

*For a discussion of the consequences for heat transfer in CVT, see paper by Rosenberger, DeLong and Olson.

HEAT TRANSFER AND TEMPERATURE OSCILLATIONS IN CHEMICAL VAPOR TRANSPORT[†]

F. Rosenberger, M. C. DeLong and J. M. Olson

Physics Department, University of Utah
Salt Lake City, Utah 84112

The temperature profile in a crystal growth system plays a crucial role in morphological stability considerations and interpretation of growth phenomena in general. In growth from vapor, particularly in closed ampoules, it is difficult to determine the actual temperature conditions. Thus, the temperature distribution of the heat source is commonly assumed to also apply to the growth system.

Temperature measurements inside a closed CVT system employing thermocouples revealed that the temperature profiles of heat source and growth ampoule can greatly deviate. Transport agents that thermally dissociate, such as $TeCl_4$[*] and I_2, can lead to sizeable heat transfer rates in a temperature gradient. Under hydrodynamically unstable conditions, temperature oscillations of $\pm 25^{o}C$ were measured in the gas phase.

A brief discussion of heat transfer mechanisms in chemical vapor transport is illustrated with measurements under different geometrical and compositional conditions.

[†] Work supported by the Advanced Research Projects Agency on Grant No. DAHC-15-71-G8.

[*] See paper on TiO_2 transport with $TeCl_4$ by Rosenberger and DeLong.

B. Hydrogen Kinetics -- Theoretical

During this period a major effort has been devoted to the study of hydrogen kinetics as a tool for the determination of electronic trapping levels. This has culminated in a quite thorough understanding of the system and its availability as a tool for the trapping level studies. The results of the work are reported in preprints 1 and 2 attached. Preprint 1 deals with the theoretical aspects of the problem and preprint 2 discusses the experimental results.

C. Hydrogen Kinetics -- Experimental

See preprint 2.

D. Devices

The problem of fabricating a reliable MOSFET structure on rutile has boiled down to three parts:

1. Finding appropriate orientations of the crystal such that the rutile substructure will not present an inherently large surface charge, and thus impede or eliminate any transistor action (i.e., gain, or even source-to-drain conductance). Transistors have been constructed successfully on the (111)- and (101)- surfaces; however, devices constructed on (001)- and (110)- surfaces have repeatedly failed. Until our fabrication procedures have been refined somewhat, we cannot say whether this behavior is an inherent property of the surface, or a difference in adsorbed impurities.

2. Finding electrode material which will not diffuse significantly

into the rutile while the sample is heated to above 500°C for several minutes to deposit the SiO_2 layer. In the early transistors, aluminum was the only material used for electrodes. This was marginally acceptable so long as the source-to-drain distance was $\geq$ 200μ. However, with the recent use of masks allowing a source-to-drain distance of 25μ, aluminum electrodes were found to diffuse quickly into the rutile and produce a low resistance path from source-to-drain. Other materials were tried, including molybdenum, copper, and gold. Molybdenum will not diffuse into the rutile even at much higher temperature, and thus appeared to be an excellent prospect. However, it oxidizes fairly rapidly while the SiO_2 is being put down; and worse yet, it appears to have rather high mobility on the surface of the rutile -- thus, shorting out the source and drain electrodes. Copper also oxidizes rapidly, forming layers of unstable and erratic conductivity. Gold will neither oxidize nor diffuse at these temperatures, but unfortunately it adheres to the rutile surface very poorly. Thus, in an attempt to make use of gold electrodes, the following procedure was devised. Initially, semi-transparent aluminum electrodes (about 50-100Å) were evaporated onto the rutile, which were then overcoated with evaporated gold. This procedure resulted in a strong, durable electrode; Al diffusion into the TiO_2 appeared to be minimal. Since it was necessary to move the sample when changing from the aluminum evaporating filament to the gold evaporating filament, a highly stable masking device was built which clamped the rutile sample over a 1-mil tungsten wire. Thus, we now have a highly reliable, reproducible way of producing a 1-mil source-to-drain separation along with rather good electrodes. Testing is proceeding on these devices.

3. Finding a way to clean the surface of the rutile to eliminate mobile charges in the SiO_2 and at the TiO_2 - SiO_2 interface. A single

monolayer of contaminants can represent a significant fraction of 1% concentration if it diffuses into a glass layer a few thousand angstroms thick, significant instabilities may develop and, in fact, this appears to be a major problem. For the present, we are attempting to solve this problem by a combination of aqueous chemical treatments and heat treating cycles. It seems likely, however, that the final solution will require fabrication of the devices in the RF sputter-etching system, which should permit us to fabricate very clean devices. Installation of this equipment has proceeded rather slowly, since we felt it was necessary to provide a very clean pumping system, but it is expected to be operational within the next month. This should coincide well with the availability of our first locally grown crystals.

E. Review Paper

1. Progress on the review paper has been slow due to the large number and complexity of published experimental results. However, a first draft is complete except for the transport and sample growth sections and a summary of defect effects. The work involved in producing the review has given rewards in the form of suggestions for useful experiments as well as new insights concerning rutile. For example, we have been able to correlate optical and phonon data which, with the optical selection rule tables generated for the review, have allowed us to conclude that the minimum band gap in rutile is an indirect gap of 3.02eV, probably involving transitions between the Γ and M points of the Brillouin zone. These results have been submitted for publication. (See Preprint III). These results have been received with considerable interest by another group here at Utah which is presently involved with band structure calculations for rutile. The reason

for the interest is that the calculated symmetry assignments are the only experimental data available which may be compared directly with the band structure calculations.

F. Far Infrared Spectroscopy

During this period construction of the spectrometer has been essentially completed with initial operation planned for September. We are setting up the following series of experiments for the initial runs.

The first experiment will be to measure over a wide range the transmission and reflectivity of the purest samples we have, as provided by our crystal growth effort. The purpose of these measurements is to establish accurate values of the transmission and reflection due to the lattice alone. This data will be stored on magnetic tape.

The second experiment will be to measure both reflection and transmission of some nominally doped samples. This data will be compared with the pure data to locate impurity induced absorption and reflection. Once we have established the locations of the impurity induced absorption and reflection, we will make high resolution and high signal-to-noise measurements to accurately determine the structure of the impurity induced absorption. Then we will diffuse in impurities to determine whether the absorption is due to a given impurity. Studies of these absorptions as a function of Fermi level (controlled as described in the Sections B and C) will follow. Study of absorptions associated with H^+ and D^+ also have a high priority; among other things, such studies might yield information on such interesting

as the exact site in the lattice of the H^+.

Another experiment in this first series will be to look at samples with conduction electrons. Small polaron theory predicts that in a perfect crystal there will be no free carrier absorption below the first interacting phonon energy. However, in imperfect crystals, detect scattering should permit us to measure free carrier absorption.

G. Magnetic Resonance

As mentioned in the previous (Nov. 1971) progress report, "Vacuum Reduction" does not occur below 1000°C. However, some reduction does take place at higher temperatures (~ 1200°C). We have analyzed the ESR and optical absorption spectra of rutile reduced in this fashion. We find an ESR spectrum similar to that found by Chester[1] for vacuum reduced material. Reoxidation appears to proceed in 2 stages. In the first stage, the re-oxidation proceeds > 90% of the way to completion as indicated by the optical absorption spectrum. However, the ESR spectrum does not change. Further oxidation is difficult but reduces the observed ESR spectrum as it proceeds. We find no evidence of Ti^{3+} interstitials and hence have looked elsewhere for the source of the spectra. All the ESR work was done at 4°K as the sample is very lossy above He temperature. See Preprint IV

In an effort to see if "vacuum reduction" is due to carbon interstitials arising from hydrocarbon contamination of dirty vacuums, a sample was reduced in $C^{13}O$. Light optical coloration of the sample was obtained, but a very strong 4°K signal was seen with $g_{\parallel} = 1.949$ and $g_{\perp} = 1.976$. No resolved hyperfine structure due to C^{13} was seen, but there is a suggestion of an unresolved splitting. ENDOR studies of this possible splitting are planned.

As mentioned in Sections B and C the Fermi-level can be moved about in the gap resulting in various charge states for defects and impurities in rutile. These slates have been identified by ESR in the case of Mo. The states are Mo^{6+}, Mo^{5+}, Mo^{4+}, and Mo^{3+} with 5+ and 3+ yielding ESR spectra. This is the first report of Mo^{3+} in rutile. The spectra for Mo^{3+} have all been taken and are being analyzed. A paper on the technique of Fermi level variation to obtain various ESR charge states will be presented at the Colloque Ampére in August, 1972.

H. Free Carrier Optical Absorption

A major unanswered question in rutile has been the origin of the extremely broad optical absorption peak centered at 1.5 μ. It is known to be associated with conduction electrons since its intensity scales with the conductivity, but the reasons for its shape are much in doubt. The most promising explanation for the peak has been put forward by Bogomolov, et al.[2] who ascribe it to a small polaron exhibiting hopping type conduction. A key prediction of their theory is that the peak should shift to higher energies as the temperature is lowered. They examined the temperature dependence of the peak in rather poorly characterized samples and did indeed observe a shift to higher energies. We have now examined the temperature dependence on well-characterized samples and find that for rutile with a Ti^{4+} interstitial concentration which is relatively high compared to the H concentration, there is indeed a noticeable shift of the carrier peak to higher energies as the temperature is lowered below 77°K. However, for rutile doped with hydrogen with a nominally small Ti^{4+} interstitial concentration, no such

peak shift is observed. Hence, while these experiments seem to confirm the localized electron transfer model for the absorption, it is not due to an intrinsic property of the lattice but rather to Ti interstitials. In this case, the peak shift corresponds to the trapping of electrons on Ti^{4+} interstitials. However, we have also found that, even at room temperature, rutile can be put in a state such that there is a considerable component of the higher energy (i.e., 1.1 eV) absorption. This occurs in crystals which have been treated specifically to eliminate all donors (particularly H) except for Ti interstitials, and in which the Ti interstitial concentration is fairly low -- presumably of the order of 1/3 the density of electron traps. If the absorption at 1.1 eV is indeed due to an electron trapped on a Ti interstitial, it is easy to understand why it has not previously been seen at room temperature, since addition of more Ti interstitials would result in a strong free carrier absorption, which would quickly mask the higher energy absorption. Thus, the 1.1 eV peak can only be observed over a very narrow range of Ti interstitial concentration, and could easily be missed except in a careful, systematic study of absorption as a function of Ti concentration.

Unfortunately, the first observation can be consistant with the proposed model only if the number of electron states available within ~ .025 eV (~ kT) of the bottom of the conduction band is comparable to the concentration of Ti interstitials, which seems rather improbable. Thus, the situation may be somewhat more complicated. Work is continuing on this problem; in particular, we plan to do correlated studies of optical absorption and AC conductivity as a function of temperature in such crystals.

I. Hydrogen Diffusion

As discussed in Section C, the work on H solubility has also provided an excellent technique for measurement of H diffusion. The general approach of isotope substitution probably provides the only sound technique for such measurements in systems where the chemical potential of a given ion is concentration dependent. Although we do not have sufficient data as yet to obtain an accurate value of the activation energy for H diffusion, we have obtained some preliminary measurements on both doped and undoped crystals, and several interesting conclusions can already be drawn. For example, we find H-diffusion is strongly inhibited by the presence of Al impurities, but much less effected by Fe. At 800°C, the diffusion coefficient for an Al doped crystal is at least 10 times smaller than for a crystal with comparable Fe concentration. (This is in qualitative agreement with the work of Hill[3], although other aspects of his work are probably not correct). It is tempting to try to account for the difference in diffusion coefficients on the basis of proton trapping near Al in the lattice, since it is known from IR measurements[4] that there is some trapping of H^+ near Al but apparently not in the case of Fe. Preliminary calculations indicate, however, that the trapping due to Al should only produce a very minor effect. Further study of this problem is planned.

Calculations indicate that the diffusion coefficients for H^+ and D^+ at 800°C should differ by approximately a factor of 2 (D^+ being slower), due to the differences in zero point energy and in the vibrational frequencies. Our measurements, as described in Section C, however, reveal no measurable difference. Indeed, we find that the total concentration of H^+ plus D^+ remains constant within experimental error, over the whole

range of isotope substitution, contrary to what would be expected on the basis of the expected difference in diffusion coefficients. Thus the results of our experiments clearly illustrate the overriding importance of factors in the driving force for diffusion other than concentration gradients -- specifically, variation in the electrostatic potential, due to space charges.

In summary, we believe we now have access to a technique which permits meaningful diffusion measurements to be made for the first time in this material and work is proceeding to exploit this technique.

J. Trapping Levels

As mentioned in Sections B and C, we have developed a technique for determining the electron trapping levels associated with a given impurity by means of the dependence of the Fermi level on equilibration temperature in an $H_2O + O_2$ atmosphere. We are currently applying this technique to Mo doped samples. As noted in Section G, we have identified the charge states associated with the optical absorptions. Thus, by monitoring the OH and optical absorptions and using the theory developed in Section B, we can determine the thermal trapping energies of each state. As seen is Section B, this requires measurement of $E_{<H^+>}$, the proton energy. We are currently measuring this by the technique of Section B. These same measurements will also yield the conduction band parameters (the energy of the conduction band minimum, E_c, and the effective density of states), thus permitting placement of all other measured energies relative to E_c. This measurement and the Mo work is currently in progress and results are expected shortly.

We are also preparing samples for similar work on W, Nb, V, and Fe doped material. In fact, it seems that the levels due to virtually any impurity and charge state can be mapped out in this fashion.

REFERENCES

1. P. F. Chester, J. Appl. Phys. 32, 2233 (1961).

2. V. N. Bogomolov, E. V. Kudinov, Yu. A. Firsov, Sov. Phys. Solid State 9, 2502 (1968).

3. G. J. Hill, Brit. J. Appl. Phys., 1, 244 (1968).

4. O. W. Johnson, W. D. Ohlsen and Paul I. Kingsbury, Jr., Phys. Rev. 175, 1102 (1968).

Preprint No. 1

DEFECT AND IMPURITY THERMODYNAMICS IN RUTILE-LIKE SYSTEMS*

John W. DeFord and O. W. Johnson
Department of Physics, University of Utah
Salt Lake City, Utah 84112

An analysis is presented of the thermodynamics of lattice defects and H or D in rutile. It is shown that the solubility of these imperfections depends strongly on electron Fermi level, which in turn depends on the concentration of the imperfections. A method is presented for using hydrogen solubility to determine conduction band parameters and the energies and densities of electron traps in the crystal. The conditions for obtaining large or small concentrations of H,D or lattice defects are discussed. The use of the method presented depends on an accurate calibration of the oscillator strengths of the H-D IR absorption in rutile. Such a calibration is presented in the following paper.

*This research supported by the Advanced Research Projects Agency under Contract No. DAHC-15-71-G8.

I. INTRODUCTION

This paper will discuss a theoretical investigation of the defect thermodynamics of rutile and similar systems. Special attention will be paid to hydrogen solubility and its application to the determination of electron trapping levels associated with impurities and lattice defects. The following paper[1] describes corresponding experimental investigations.

The solubility of H or of a lattice defect is complicated by the fact that the Fermi level - μ_e - can be widely varied (in principle, over the entire band gap of about 3 eV[2]). This means that there will not be a unique "binding energy" for an electrically active impurity or defect in rutile, since the effective binding energy includes both the ion energy (presumably a constant) and that of its valence electrons (which enter the lattice at μ_e, which is variable). Hence, there is no unique solubility for such impurities or defects in rutile. We will develop a complete thermodynamic description of the system, including arbitrary impurities and defects, subject to assumption that the concentrations are low enough that the perfect crystal band structure is not altered (an assumption nearly always satisfied in practice). We also identify the parameters necessary to characterize the systems and indicate how they may be evaluated experimentally.

In particular we are concerned with predicting μ_e and the concentrations of H and Ti interstitials which will result from various heat treatments and atmospheres. These two entities were chosen for detailed analysis because H makes a very convenient, reversible dopant for probing electronic properties, and Ti interstitials appear to be the dominant defect and

hence will generally be important in establishing equilibrium. We will also show that direct and relatively simple measurements will suffice to determine the trapping levels and concentration of any particular impurity or lattice defect. We will derive expressions for the dependence of electron Fermi level on these parameters and hence the theory will allow prediction of the treatment required to produce a crystal with any desired μ_e. We will show that the key to this technique lies in an accurate measurement of H concentration and that this can be done by measurement of the IR absorption[3] associated with H, once an accurate calibration factor is determined. The following paper[1] includes such a calibration.

In spite of the rather extensive effort that has been devoted to the behavior of lattice defects and H in the rutile system,[4,5] there remains considerable ambiguity and much misunderstanding as to the conditions under which hydrogen and/or lattice defects will diffuse into the rutile lattice. To indicate the complexity of the system, we will show that heating in an atmosphere of H_2O and O_2 results in a high concentration of H in the lattice, while heating in a dry H_2 atmosphere generally results in virtually no H in the crystal. H is an electron donor in TiO_2, and hence as mentioned above the concept of a unique "solubility" for H in rutile is meaningless until μ_e is specified. The problem is further complicated by the fact that μ_e obviously depends on the H concentration as well as on the concentration of all other electrically active impurities, some of which are also mobile at the temperatures involved in H diffusion. It is worth noting that the large band gap in rutile allows large changes in μ_e, which can change solubilities (not only of H, but other species as well) by many orders of magnitude. This fact has been overlooked by many investigators and has frequently resulted in misinterpretation of results. It is, however,

this dependence of H solubility on μ_e, and hence on electron trapping levels, that makes it a powerful tool in the analysis of impurities, as will be shown below.

In Section II we discuss in detail the theory of H solubility, the determination of impurity trapping levels and conduction band density of states effective mass, and the distinction between the energies measured by optical absorption and thermal energies, due to the polaron nature of rutile.[6] Possible applications of this technique to various rutile-impurity systems are discussed in Section III.

II. THEORY

We will now consider the equilibrium concentration of H in rutile in the presence of an atmosphere of O_2, H_2, and H_2O at elevated temperatures. It is known that rutile becomes oxygen deficient when heated in the presence of H_2.[7] This could result, in principle, from the production of either O vacancies or Ti interstitials. The preponderance of evidence supports the latter interpretation, at least at temperatures below 1000°C[8], and we will assume that Ti interstitials are the dominant defect. However, the analysis is readily modified to allow for O vacancies, without qualitative change in our essential conclusions.

We suppose that the system consists of the following species: H_2O, H_2, O_2, TiO_2, $<Ti^{4+}>$, $<H^+>$, e- where $<Ti^{4+}>$ denotes a titanium interstitial e- denotes an electron, and $<H^+>$ denotes an interstitial proton. The valence of the Ti interstitial has received considerable attention and it may be that the last word has not yet been said on this matter.

The preponderance of evidence is, however, that the charge is "normally" 4+, although there is apparently a shallow electron trap associated with this defect.[8] We assume that this trap is sufficiently shallow that it is essentially unpopulated at the temperatures in question. The minor modification of our treatment which would be required if this assumption proves to be incorrect is again straightforward.

The following reactions are then possible:

$$2H_2(g) + TiO_2 \leftrightarrow 2H_2O(g) + \langle Ti^{4+} \rangle + 4e^- \quad (1)$$

$$2H_2O(g) \leftrightarrow 4\langle H^+ \rangle + 4e^- + O_2(g) \quad (2)$$

$$2H_2O(g) \leftrightarrow 2H_2(g) + O_2(g) \quad (3)$$

$$H_2(g) \leftrightarrow 2\langle H^+ \rangle + 2e^- \quad (4)$$

$$TiO_2 \leftrightarrow O_2(g) + \langle Ti^{4+} \rangle + 4e^- \quad (5)$$

Eq. (5) can be obtained from Eqs. (1) and (3), so these are obviously not all independent, but it is convenient to list all possibilities.

The condition for equilibrium at constant temperature and pressure is that the total Gibbs Free Energy for the system be a minimum. We will assume that the $\langle H^+ \rangle$ and $\langle Ti^{4+} \rangle$ do not interact, except through their influence on μ_e. This is probably not correct under all circumstances, at least for the $\langle Ti^{4+} \rangle$, since there is some evidence for the formation of complexes.[9] Since there is no detailed information available on these complexes, it is futile to attempt to treat them at this point. Our treatment should be correct at low concentrations, however, and can be readily modified when experimental data on these complexes become available. With this assumption, the condition on the Gibbs Free Energy can be replaced by the condition that the Gibbs Free Energy for each of the reactions (1) -

(5) be simultaneously a minimum. Then,

$$\sum_{i=1}^{7} \left(\frac{\partial G}{\partial N_i}\right)_{T,P,N} dN_i \equiv \sum_{i=1}^{7} \mu_i dN_i = 0 \quad , \tag{6}$$

where the derivative is taken with temperature, pressure, and all N except N_i constant. N_i denotes the number of particles of species i, and μ_i is its chemical potential. (Note that throughout we have treated the system in terms of total numbers of each specie, rather than concentrations.) The sum runs over the 7 species listed above. It is well known that μ_i can also be written as

$$\mu_i = \left(\frac{\partial F}{\partial N_i}\right)_{T,V,N} , \tag{7}$$

and that:

$$F = -kT \log Z \tag{8}$$

where Z is the partition function:

$$Z = \sum_j \exp[-\epsilon_j/kT], \tag{9}$$

where ϵ_j is the energy of the j^{th} state (see appendix A), k is Boltzmann's constant, T is the absolute temperature, and the sum is over all states of the system. Imposing the requirement that the total number of each chemical specie is constant leads to the set of equations:

$$2\mu_{H_2} + \mu_{TiO_2} - 2\mu_{H_2O} - \mu_{<Ti^{4+}>} - 4\mu_e = 0 \tag{10}$$

$$2\mu_{H_2O} - 4\mu_{<H^+>} - 4\mu_e - \mu_{O_2} = 0 \tag{11}$$

$$2\mu_{H_2O} - 2\mu_{H_2} - \mu_{O_2} = 0 \tag{12}$$

$$\mu_{H_2} - 2\mu_{<H^+>} - 2\mu_e = 0 \tag{13}$$

$$\mu_{O_2} + \mu_{<Ti^{4+}>} + 4\mu_e - \mu_{TiO_2} = 0 \tag{14}$$

Equations (10) → (14), when accompanied by expressions for the various chemical potentials, completely determine the equilibrium of the system. In particular, they permit calculation of the $<H^+>$ and $<Ti^{4+}>$ concentrations in equilibrium with a given atmosphere at any temperature and pressure.

The chemical potentials are either known or readily calculated except for μ_e and μ_{TiO_2}. Details are given in Appendix A. The results are:

$$\mu_{H_2O} = kT \log P_{H_2O} - \gamma_{H_2O} \tag{15}$$

$$\mu_{H_2} = kT \log P_{H_2} - \gamma_{H_2} \tag{16}$$

$$\mu_{O_2} = kT \log P_{O_2} - \gamma_{O_2} \tag{17}$$

$$\mu_{<H^+>} = - E_{<H^+>} + kT \log N_{<H^+>} \tag{18}$$

$$\mu_{<Ti^{4+}>} = - E_{<Ti^{4+}>} + kT \log N_{<Ti^{4+}>} \tag{19}$$

$$\mu_{TiO_2} = - E_{TiO_2} + \gamma_{TiO_2} \tag{20}$$

where the γ's are functions only of temperature and are defined in Appendix A. The P's are partial pressures in dynes/cm^2. μ_e is the electron Fermi level in the crystal and depends on the impurities and defects present (see below and Appendix B). $E_{<H^+>}$, $E_{<Ti^{4+}>}$ and E_{TiO_2} are also defined in

Appendix A.

It is convenient now to consider two special cases in which $P_{H_2} >> P_{H_2O}$, P_{O_2}, and in which $P_{H_2O} \sim P_{O_2} >> P_{H_2}$.

From Equations (10) → (20) we find: For $P_{H_2} >> P_{O_2}$, P_{H_2O}

$$N_{<H^+>} = P_{H_2}^{\frac{1}{2}} \exp\left[\frac{2E_{<H^+>} - 2\mu_e - \gamma_{H_2}}{2kT}\right] \tag{21}$$

$$\frac{N_{<H^+>}}{N_{<Ti^{4+}>}} = \frac{(P_{H_2O})^2}{(P_{H_2})^{3/2}} F(T) \exp(3\mu_e/kT) \tag{22}$$

where $$F(T) \equiv \exp\left[\frac{-2\gamma_{H_2O} - \gamma_{TiO_2} + 3/2\,\gamma_{H_2} - E_{<Ti^{4+}>} + E_{TiO_2} + E_{<H^+>}}{kT}\right]. \tag{23}$$

For $P_{H_2O} \sim P_{O_2} >> P_{H_2}$

$$N_{<H^+>} = \frac{P_{H_2O}^{\frac{1}{2}}}{P_{O_2}^{\frac{1}{4}}} \exp\left[\frac{\gamma_{O_2} - 2\gamma_{H_2O} + 4E_{<H^+>} - 4\mu_e}{4kT}\right] \tag{24}$$

$$\frac{N_{<H^+>}}{N_{<Ti^{4+}>}} = (P_{O_2})^{3/4} (P_{H_2O})^{1/2} g(T) \exp(3\mu_e/kT), \tag{25}$$

where

$$g(T) \equiv \exp\left[\frac{-\gamma_{TiO_2} - \frac{3}{4}\gamma_{O_2} - \frac{1}{2}\gamma_{H_2O} + E_{<H^+>} + E_{TiO_2} - E_{<Ti^{4+}>}}{kT}\right] \tag{26}$$

From Equations (21)→ (26) one sees that use of a dry H_2 atmosphere (such as would be obtained with use of a cold trap) produces $<Ti^{4+}>$ rather than $<H^+>$, whereas an atmosphere of H_2O +O_2 produces $<H^+>$ - a somewhat

surprising result. As discussed in the following paper, this prediction is borne out experimentally.

From Equation (24), it is clear that a measurement of $N_{<H^+>}$ for given T, P_{H_2O}, and P_{O_2} determines $(E_{<H^+>} - \mu_e)$. If we can determine $\mu_e - E_c$ for the same sample we can then combine the two equations to get $E_{<H^+>} - E_c$. Then, since E_c can be determined from the known work function,[10] we obtain $E_{<H^+>}$.

To get the relation between μ_e and E_c we need the form of μ_e, (i.e., its dependence on temperature, electron concentration, and conduction band parameters). This can be found by an extension of the work of Shockley and Last[11], which requires detailed knowledge of the electron energy levels in the crystal, including the conduction band states and any trapping levels lying in the gap. Experimentally, many impurities can exist in rutile in a variety of different charge states[12]. Hence, μ_e must be calculated for trapping levels due both to ions of two charge states (i.e., filled or unfilled) and of many charge states (multiple trapping levels). For concreteness we consider two impurities -- one with only two charge states and one with several. We suppose that each ionic charge state can also occur in several energy levels denoted by E_{si} where the index s refers to the charge and the index i to the energy levels of a particular charge state. We suppose also that the conduction band can be characterized by a density of states effective mass, m^*. Then if n_e is the number of non-valence electrons we have: (see Appendix B for details)

$$n_e = \frac{N_1}{1+\left[\frac{e^{-\beta\mu_e}\sum_i e^{-\beta E_{oi}}}{\sum_i e^{-\beta E_{1i}}}\right]}$$

$$+ \frac{N_2 \sum_{s=o}^{m} s e^{\beta\mu_e s} \sum_i e^{-\beta E_{si}}}{\sum_{s=o}^{m} e^{\beta\mu_e s} \sum_i e^{-\beta E_{si}}}$$

$$+ \frac{V}{2\pi^2}\left(\frac{2m^*kT}{\hbar^2}\right)^{3/2} \int_o^{\infty} \frac{y^{1/2}dy}{1+e^{y}e^{\beta(E_c - \mu_e)}} \qquad (27)$$

where:

N_1 = number of ions with only two charge states

N_2 = number of ions with m + 1 charge states

$\beta = \frac{1}{kT}$

V = volume of the crystal

$\hbar$ = Planck's constant /2π

E_c = energy of the conduction band minimum

For Equation (27), the energies are measured relative to a state in which the electron is removed infinitely far from the crystal (i.e., the "vacuum level").

Equations (24) and (27) can now be used to determine m and $(E_{<H^+>} - E_c)$. Consider a sample doped so that there are many trapping levels $\gtrsim$ 1 eV below the conduction band but very few near it. (Al or Fe doped

crystals without $<Ti^{4+}>$ apparently satisfy this criterion, for example). Then for fixed $N_{<H^+>}$, the number of conduction electrons will not change significantly over a temperature range from 300°K to 900°K. Hence, measurements of n_c (the number of conduction electrons) at room temperature will also yield the number present at the elevated temperature at which the system was equilibrated. From Equation (27) we have:

$$n_c = VK(T)^{3/2}I \tag{28}$$

where:

$$K = \left(\frac{2m^* k}{\hbar^2}\right)^{3/2} \tag{29}$$

and

$$I = \int_0^\infty \left[\frac{y^{1/2}dy}{e^{y_e}e^{\beta(E_c - \mu_e)}+1}\right] \tag{30}$$

For the region of low n_c (i.e., $E_c - \mu_e >> kT$), I can be approximated as:

$$I = \frac{\sqrt{\pi}}{2}\, e^{-\beta(E_c - \mu_e)} \tag{31}$$

Equations (28) and (31) yield the following relation for μ_e:

$$\mu_e = E_c + kT \log \left[\frac{2n_c}{K(T)^{3/2}\sqrt{\pi}\, V}\right]. \tag{32}$$

This provides the relation between μ_e and E_c which we sought. Equation (24) can be written in the form:

$$\mu_e = E_{<H^+>} + \tfrac{1}{2}\gamma_{O_2} - \tfrac{1}{2}\gamma_{H_2O} + kT \log \left(\frac{P_{H_2O}^{1/2}}{P_{O_2}^{1/4}}\right) - kT \log N_{<H^+>} \tag{33}$$

$$\equiv E_{<H^+>} - kT \log (N_{<H^+>}) + h(T) \quad . \tag{34}$$

Equations (32) and (34) now yield:

$$n_c N_{<H^+>} = K \exp\left(\frac{E_{<H^+>} - E_c}{kT}\right) L(T) \tag{35}$$

where:

$$L(T) = \frac{T^{\frac{3}{2}} \sqrt{\pi}\, V}{2} \exp\left[\frac{h(T)}{kT}\right] \tag{36}$$

Hence, measurements of the product $n_c N_{<H^+>}$ at two different T's is sufficient to determine K and $(E_{<H^+>} - E_c)$. (See Appendix C for details).

The work function of rutile is known,[10] so E_c is determined. Thus $E_{<H^+>}$ can be determined. Once $E_{<H^+>}$ is determined, μ_e can be found from Equation (24) for any particular experiment. In cases where the fractional occupation of any particular trapping level can be determined from the optical absorption spectrum, Equation (27) can be used to determine the energy of the level. This method will work for levels separated by >> kT, which requirement can be satisfied in almost all cases. The same information can obviously also be obtained by carefully monitoring $<H^+>$ concentration as a function of equilibrium temperature and pressures since $N_{<H^+>}$ depends on μ_e (Eqn. (24)) and μ_e depends on the energy of the trapping level (Eqn. (27)). Again all that is required is that only one level be changing population at a time ($\Delta E >> kT$). Note that this method is often more useful since it eliminates the need to carefully resolve the absorption peaks.

It must be noted that the resulting energy differences between trapping levels and the conduction band will not be the same as the optical absorption energies since the former is the energy difference between "relaxed"

(polaron) states and the latter is the energy of a transition between a "relaxed" state and an "unrelaxed" (i.e., rigid lattice) state.

Once K and $E_{<H^+>}$ are known, it is possible to systematically determine the trapping levels of virtually any impurity relative to E_c. By applying Equations (21) - (23) to a case in which the trapping levels have been determined and μ_e is close enough to the conduction band that it can be calculated from a measurement of n_c, $E_{<Ti^{4+}>}$ can be determined.

III. APPLICATIONS

In this section we discuss applications of the theory of Section II to three sample problems:

1. Minimizing $<Ti^{4+}>$ concentration.
2. Maximizing $<H^+>$ without producing conduction electrons or $<Ti^{4+}>$.
3. Determination of the trapping levels of an impurity with several charge states, e.g., Mo.

The first two problems arise in the determination of $<H^+>$ oscillator strength as discussed in Ref. (1). The third is of central importance in any investigation of the electrical properties of the crystal.

To determine the conditions of minimum equilibrium $<Ti^{4+}>$ concentration, we combine Equations (24) and (25) to obtain

$$N_{<Ti^{4+}>} = P_{O_2}^{-1} \exp[(\gamma_{O_2} - E_{TiO_2} + E_{<Ti^{4+}>} + \gamma_{TiO_2})/kT] \exp[-4\mu_e/kT] \quad (37)$$

Examination of Eqn. (37) makes it clear that a large O_2 pressure and a high Fermi level is required to eliminate $<Ti^{4+}>$. The temperature dependence of

$N_{<Ti^{4+}>}$ is also contained in Eqn. (37), but is more complicated. In practice[1] it turns out that the main concern is to use a high enough temperature that equilibrium is reached in a reasonably short time. This of course is determined by diffusion times. Since practical considerations limit attainable values of P_{O_2}, we require a means of producing a high μ_e. This can be done by introducing <H+>. Hence we are led to the question of how to maximize $N_{<H+>}$, in the presence of an O_2 atmosphere.

The best conditions for introducing <H+> can be seen from Equation (24). It is clear that we need a large H_2O pressure. The O_2 pressure dependence is weaker than in the $<Ti^{4+}>$ case. Hence the optimum conditions for minimizing $<Ti^{4+}>$ (while also maintaining a relatively high $N_{<H^+>}$ level) are to equilibrate the sample in high partial pressures of both O_2 and H_2O. As discussed in Reference (1), this technique does indeed produce a large <H+> concentration and vanishingly small $<Ti^{4+}>$ concentration.

The determination of trapping levels is a particularly important application of the theory. For concreteness, consider a sample doped with an impurity having 4 charge states, each of which has only one energy level. (In practice Mo has 4 charge states, as determined by ESR measurements to be published elsewhere, but the charge states have more than one energy level. This is a non-essential complication which will be dealt with in a subsequent publication). We suppose that the experimental conditions are such that there are no conduction electrons. Then Equation (27) becomes:

$$n_e = \frac{N_{Mo}\left[e^{-\beta(E_1-E_o-\mu_e)} + 2e^{-\beta(E_2-E_o-2\mu_e)} + 3e^{-\beta(E_3-E_o-3\mu_e)}\right]}{1 + e^{-\beta(E_1-E_o-\mu_e)} + e^{-\beta(E_2-E_o-2\mu_e)} + e^{-\beta(E_3-E_o-3\mu_e)}} \qquad (38)$$

where N_{Mo} is the number of Mo ions (assumed constant) and E_i is the energy of the i^{th} charge state. Note that E_{i+1} differs from E_i by the energy of the added electron plus any rearrangement that takes place among the lower lying electrons on the ion. Hence, roughly speaking the $(i+1)^{th}$ level will be partially filled if $E_i + \mu_e \approx E_{i+1}$. Note that this is a different type of energy level scheme than is normally encountered. (See the discussion below relating E_i to E_c). The range in values of μ_e for which a level is partially filled is ~ kT. Hence if the levels are separated by many kT, only one level will be partially filled at a time. This is the key to the method. Consider the case in which $E_1 + \mu_e \approx E_2$. Then level E_2 will be partially filled, $E_o + \mu_e$ will be $>> E_1$, and $E_2 + \mu_e$ will be $<< E_3$. Hence Equation (39) becomes:

$$n_e \simeq \frac{N_{Mo}\left[1 + 2e^{-\beta(E_2-E_1-\mu_e)}\right]}{1 + e^{-\beta(E_2-E_1-\mu_e)}} \tag{39}$$

Now if the experiment is performed under conditions which keep the $\langle Ti^{4+}\rangle$ concentration low (high P_{O_2} and moderate temperatures) all of the electrons must be provided by $\langle H^+\rangle$. Hence we can set $n_e = n_{\langle H^+\rangle}$. Referring to Equation (24) we see that measurement of $N_{\langle H^+\rangle}$ determines μ_e. In fact:

$$e^{\beta\mu_e} = \frac{(P_{H_2O})^{\frac{1}{2}}}{(P_{O_2})^{\frac{1}{4}}} \quad \frac{\exp\left[\frac{\gamma_{O_2} - 2\gamma_{H_2O} + 4E_{\langle H^+\rangle}}{4kT}\right]}{N_{\langle H^+\rangle}}$$

$$\equiv \frac{(P_{H_2O})^{\frac{1}{2}}}{(P_{O_2})^{\frac{1}{4}}} \quad \frac{J(T)}{N_{\langle H^+\rangle}} \tag{40}$$

Combining Equations (39) and (40) yields:

$$e^{\beta(E_2-E_1)} = \left[\frac{2N_{Mo} - N_{<H+>}}{N_{<H+>} - N_{Mo}}\right] \frac{(P_{H_2O})^{\frac{1}{2}}}{(P_{O_2})^{\frac{1}{4}}} \frac{J(T)}{N_{<H+>}}$$

$$= \left(\frac{2X - 1}{1-X}\right) \frac{(P_{H_2O})^{\frac{1}{2}}}{(P_{O_2})^{\frac{1}{4}}} J(T) \qquad (41)$$

where $X = \frac{N_{Mo}}{N_{<H+>}}$. Now X can be determined at any point from a plot of $N_{<H+>}$ vs T_{equil}, where T_{equil} is the equilibration temperature. Such a plot is shown schematically in Fig. 1. By measuring the height of a step we obtain N_{Mo}, and hence we can determine X at any point on the curve. Thus $E_2 - E_1$ is determined. A similar treatment of the other steps will yield all the energy differences. (In practice, it may be more feasible to vary parameters other than T_{equil}, but similar results obtain.) There remains only the question of where the levels E_i lie with respect to the conduction band. The pertinent question is how much energy is required to convert from E_3 to E_2 plus an electron in the conduction band? Let that energy be Δ. Then

$$E_3 + \Delta = E_2 + E_c \quad .$$

Thus:

$$\Delta = E_2 + E_c - E_3.$$

Now $E_2 - E_3$ is known as shown above. E_c is known as discussed in section II. Hence Δ is determined and all levels are placed with respect to the conduction band.

This technique is currently being applied to a variety of transition metal impurities in TiO_2; results will be reported in future publications.

IV. SUMMARY

We have presented a method for determining conduction band density of states effective mass and solubilities, binding energies, and trapping levels of various impurities in rutile and similar systems. The method relies on an accurate determination of the <H+> oscillator strength. Such a determination is presented in the following paper, Ref. 1.

V. ACKNOWLEDGMENT

The authors are grateful for helpful discussions with Drs. Frank Harris and Larry Scott on the statistical mechanics treatment, and to Mr. Su Pack for careful checking of the numerical work.

Appendix A

The partition functions of gases can be factored into translation, rotation, vibration and electronic parts[13]. The translation part can be treated classically at the temperatures of interest and is

$$Z_{trans} = \frac{V}{h^3} (2\pi mkT)^{3/2} \qquad (1A)$$

In the cases of H_2, O_2, H_2O, only the ground electronic state contributes. Hence:[13]

$$Z_{elect} = r_o e^{-\varepsilon_g/kT} \qquad (2A)$$

where r_o is the degeneracy of the ground state and ε_g is the energy of the ground state. The vibrational part involves a sum over harmonic oscillator energy levels for each vibrational mode. In the cases of H_2 and O_2, only the ground vibrational state contributes. Hence the zero point energy and the electronic ground state energy combine to give the dissociation energy and thus:

$$Z_{elect} Z_{vib} = r_o e^{\varepsilon_D/kT} \qquad (3A)$$

where ε_D is the dissociation energy. In the case of H_2O, the first excited states of the 3 normal modes also contribute and yield:[14]

$$Z_{elect}\, Z_{vib} = r_o e^{\varepsilon_D/kT} \left(\frac{1}{1-e^{\frac{-2296}{T}}}\right) \left(\frac{1}{1-e^{\frac{-5253}{T}}}\right) \qquad (3A')$$

$$\left(\frac{1}{1-e^{\frac{-5404}{T}}}\right)$$

Finally, the rotational parts are complicated by the symmetries of the nuclei. However, they are well understood and yield [13] (at ~ 300°C and above):

$$Z_{Rot_{O_2}} = 2.431 \times 10^{-1} T$$

$$Z_{Rot_{H_2O}} = 3.358 \times 10^{-2} T^{\frac{3}{2}} \qquad (4A')$$

$$Z_{Rot_{H_2}} = 2.424 \times 10^{-2} T \qquad (4A'')$$

Combining Equations (1A) → (4A'') with Equations (7) and (8) yields:

$$\gamma_{O_2} = + 1.380 \times 10^{-16} T \log \{3.421 \times 10^{6} e^{\frac{5.896 \times 10^{4}}{T}} T^{\frac{7}{2}} \} \qquad (5A)$$

$$\mu_{O_2} = kT \log P_{O_2} - \gamma_{O_2} \qquad (5A')$$

$$\gamma_{H_2O} = 1.380 \times 10^{-16} T \log \{6.645 \times 10^{4} e^{\frac{1.111 \times 10^{5}}{T}} T^{4} \left(\frac{1}{1-e^{\frac{-2296}{T}}}\right) \left(\frac{1}{1-e^{\frac{-5253}{T}}}\right) \left(\frac{1}{1-e^{\frac{-5404}{T}}}\right)\} \qquad (6A)$$

$$\mu_{H_2O} = kT \log P_{H_2O} - \gamma_{H_2O} \qquad (6A')$$

$$\gamma_{H_2} = 1.380 \times 10^{-16} T \log \{5.330 \times 10^{3} e^{\frac{5.195 \times 10^{4}}{T}} T^{\frac{7}{2}} \} \qquad (7A)$$

(7A')

$$\mu_{H_2} = kT \log P_{H_2} - \gamma_{H_2}$$

The partition functions for $\langle H^+ \rangle$ and $\langle Ti^{4+} \rangle$ are found by assuming that each has but one state in the crystal. This is not quite true in the case of $\langle H^+ \rangle$ as shown by slightly displaced, impurity-associated absorption peaks[15]. This assumption is a good approximation, however, and can easily be removed if necessary. We chose as a standard state -- the zero of energy -- the state of separated H atoms, O atoms, and Ti atoms. We will, however, measure electron energies relative to the state in which they are infinitely separated from everything ("vacuum" level).

Consider $\langle H^+ \rangle$. Starting with the standard state we produce $\langle H^+ \rangle$ as follows: First remove the electron. This requires energy E_R. Next, insert the electron in the crystal. This takes energy μ_e. Then insert the proton in the crystal. This requires energy E_p. Thus the total energy required to produce $\langle H^+ \rangle$ from the standard state is:

$$E_p + E_R + \mu_e$$

(Note that both E_p and μ_e are negative numbers).
We chose to treat the electrons separately. Hence, let

(8A)

$$-\langle E_{H^+} \rangle = E_R + E_p$$

Consider $\langle Ti^{4+} \rangle$. To produce a $\langle Ti^{4+} \rangle$ we must remove 4

electrons. This takes an energy $E_1 + E_2 + E_3 + E_4$. We then place the 4 electrons in the crystal. This requires an energy $4\mu_e$. We then insert the Ti^{4+} in the lattice. This takes an energy E_T. Hence the total energy required to make a $<Ti^{4+}>$ is

$$E_1 + E_2 + E_3 + E_4 + 4\mu_e + E_T \ .$$

Again we treat the electrons separately and define

(9A)

$$-E_{<Ti^{4+}>} = E_1 + E_2 + E_3 + E_4 + E_T \ .$$

We can now calculate the partition functions from Equations (7) -(9). We have

$$Z = \frac{(e^{E/kT})^N}{N!}$$

$$F = - kT \{N \frac{E}{kT} - N \log N + N\}$$

$$\mu = - E + kT \log N$$

Hence:

(10A)

$$\mu_{<H^+>} = -E_{<H^+>} + kT \log N_{<H^+>}$$

(11A)

$$\mu_{<Ti^{4+}>} = -E_{<Ti^{4+}>} + kT \log N_{<Ti^{4+}>} \ .$$

We can calculate μ_{TiO_2} in the solid state as follows. We have

$$C_V = -T \frac{\partial^2 F}{\partial T^2})_V$$

Hence:

$$\int_o^T \frac{C_V}{T}\, dT = -\int_o^T \frac{\partial}{\partial T})_V \frac{\partial F}{\partial T})_V\, dT$$

$$= -\frac{\partial F}{\partial T})_V \Big|_T + \frac{\partial F}{\partial T})_V \Big|_0$$

$$= -\frac{\partial F}{\partial T})_V \Big|_T - S(0)$$

where S(0) is the entropy at 0°K. Let

$$-A \equiv \int_o^T \frac{C_V}{T}\, dT \qquad (12A)$$

where C_V is the specific heat at constant volume. Then

$$\int_o^T \frac{\partial F}{\partial T})_V\, dT = \int_o^T [A - S(0)]\, dT$$

$$F(T,V) - F(0,V) = -S(0)T + \int_o^T A\,dT \,. \qquad (13A)$$

Now let $-E_{TiO_2}$ be the energy of the ground state of a TiO_2 molecule in the crystal relative to the standard state.

Then,

(14A)

$$F(0,V) = - NE_{TiO_2}$$

where N is the number of TiO_2 molecules in the solid. Letting

(15A)

$$C_V = \overline{C}_V N$$

where $\overline{C}_V$ is the specific heat per molecule, and noting that S(0) = 0 we find

(16A)

$$\mu_{TiO_2} = -E_{TiO_2} + \gamma_{TiO_2}$$

where

(17A)

$$\gamma_{TiO_2} = -\int_0^T dT' \int_0^{T'} \frac{\overline{C}_V(T'')}{T''} dT''$$

Appendix B

The chemical potential for N electrons is

$$Z_e(N) = \sum_i e^{-\beta\epsilon_i} \tag{1B}$$

subject to the restriction that

$$\sum_i n_i = N \tag{2B}$$

where the sum is over all states of the system. The restriction can be removed in the usual way[16] by calculating instead the function z_e given by

$$z_e = \sum_{N'} Z_e(N') e^{-\gamma_e N'} \tag{3B}$$

and choosing γ_e so that $Z_e(N')e^{-\gamma_e N'}$ has a maximum at $N' = N$. Then

$$\log z_e = \log Z_e(N) - \gamma_e N \tag{4B}$$

$$F = -kT \log Z_e(N) = -kT \log z_e - kT\,\gamma_e N\,. \tag{5B}$$

Thus,

$$\mu_e = -kT\,\gamma_e \tag{6B}$$

The condition on γ_e leads readily to the relation

$$N = - \frac{d \log z_e}{d\gamma_e} \tag{7B}$$

We will assume that the impurities are independent (except for their effect on μ_e). Then the partition function factors into terms for the conduction band and for each of the impurities. Thus,

$$\log z_e = \log z_1 + \log z_2 + \log z_{cond} \, . \tag{8B}$$

Now, since each impurity ion is assumed independent, the partition function for a given kind of ion factors into terms for each individual ion. This means that

$$z_i = (z)^{N_i} \tag{9B}$$

where z is the partition function for a single ion and N_i is the number of ions. Thus,

$$\log z_i = N_i \log \sum_{s=0}^{m} e^{\beta\mu_e s} \sum_j e^{-\beta E_{sj}} \, . \tag{10B}$$

Equations (6B), (7B), (8B), and (10B) can then be combined to yield Equation (27). The conduction band term in (27) arises from ordinary Fermi-Dirac statistics[17].

Appendix C

To determine the values of K and $E_{<H^+>}$, imagine measurements of $N_{<H^+>}$ n_c at two temperatures, T_1 and $T_1 + \Delta$. Equation (35) then yields

$$E_{<H^+>} - E_c = \frac{k(T_1 + \Delta)T_1}{\Delta} \ln \left[\frac{L(T_2)}{L(T_1)} \frac{(n_c N_{<H^+>})_1}{(n_c N_{<H^+>})_2}\right] \tag{1C}$$

$$K = \frac{(n_c N_{<H^+>})_1}{L(T_1)} \left[\frac{L(T_1)(n_c N_{<H^+>})_2}{L(T_2)(n_c N_{<H^+>})_1}\right]^{\left(\frac{T_1 + \Delta}{\Delta}\right)} \tag{2C}$$

where $T_2 = T_1 + \Delta$ and $(n_c N_{<H^+>})_1$ refers to the value at T_1, and $(n_c N_{<H^+>})_2$ refers to the value at T_2.

References

1. O. W. Johnson and J. W. DeFord, "An Experimental Method for the Exact Determination of Hydrogen Concentration in Rutile," (following article).
2. J. W. Shaner, Phys. Rev. Letters (to be published).
3. A. Von Hippel, J. Kalnajs, W. B. Westphal, J. Phys. Chem. Solids 23 779 (1962).
4. M. G. Harwood, Special Ceramics 4 (P. Popper, ed.) 1968, p. 213.
5. G. J. Hill, Brit. J. Appl. Phys. 1, 1151 (1968).
6. V. N. Bogomolov, E. V. Kudinov, Yu. A. Firsov, Sov. Phys. Solid State 9, 2502 (1968).
7. F. A. Grant, Rev. Mod. Phys. 31, 646 (1959).
8. Paul I. Kingsbury, Jr., W. O. Ohlsen, and O. W. Johnson, Phys. Rev. 175 No. 3, 1091-1098 (1968).
9. J. B. Wachtman, L. R. Doyle, Phys. Rev. A135, 276 (1964).
10. W. E. Spicer and G. F. Derbenwick (unpublished).
11. W. Shockley and J. T. Last, Phys. Rev. 107, 392 (1957).
12. W. Low, and E. L. Offenbacher, Solid State Physics 17, (1965).
13. Joseph E. Mayer, Handbuck Der Physik, Vol 12 pages 73-123, Springer Verlag, Berlin, 1958.
14. D. M. Dennison, Rev. Mod. Phys. 12, 175 (1940).
15. O. W. Johnson, W. D. Ohlsen, and Paul I. Kingsbury, Jr., Phys. Rev. 175 No. 3, 1102-1109 (1968).
16. F. Reif, Statistical and Thermal Physics, pages 346-349, McGraw Hill, New York, 1965.
17. C. Kittel, Introduction to Solid State Physics, 3rd Edition, page 209, Wiley, New York, 1968.

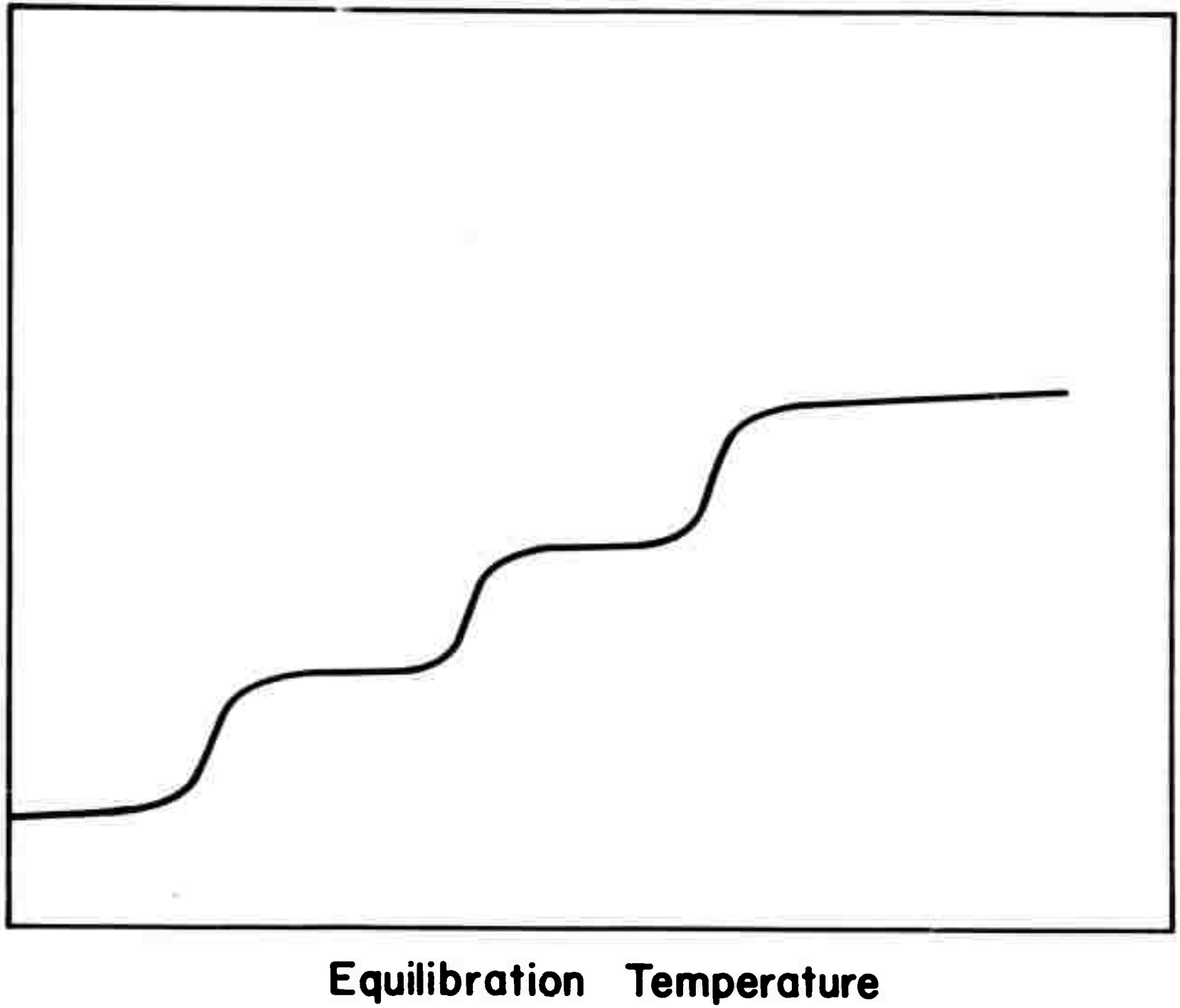

Fig. 1: $\langle H^+ \rangle$ concentration vs equilibration temperature for a crystal containing A level acceptors, such as Mo substitutionals

Preprint No. 2

"An Experimental Technique for the Precise Determination of H and D Concentration in Rutile (TiO_2)."*

O. W. Johnson and John DeFord
Department of Physics, University of Utah
Salt Lake City, Utah 84112

Results of a precise determination of the IR absorption strength of H and D in rutile are presented, which permit determination of H or D concentration to an accuracy of 3%. Used in conjunction with the results of the theoretical analysis of the preceding paper[1], this technique makes possible the accurate determination of the energy and density of all electron trapping levels in TiO_2 crystals. Several previously unreported satellite spectra for both H and D are described and possible identifications are discussed. A technique for measuring diffusion parameters of H and D under conditions of strict chemical equilibrium, thus avoiding the large departures from Fick's law which usually plague such measurements in materials such as TiO_2, is also described.

*This research supported by the Advanced Research Projects Agency under Contract No. DAHC-15-71-G8.

I. Introduction

The preceding paper[1] outlines a method of analysis by means of which the complete equilibrium "defect thermodynamics" of a system such as rutile can be derived from measurements of the solubility of H as a function of equilibration temperature and partial pressures. By this we mean that the electron energy levels and densities of all electron traps can be determined for a crystal containing unknown impurities, or alternatively, the electronic structure and H solubility of a crystal of known doping can be calculated. In addition, the analysis permits calculation of the equilibrium concentration of Ti interstitials (which we assume to be the dominant lattice defect and will hereafter denote as $\langle Ti^{4+} \rangle$)and an independent measurement of the conduction band effective mass (or the conduction band effective density of states). The importance of these parameters in characterizing a semiconductor for device applications (either electronic or electro-optical) or in achieving a fundamental understanding of the material, is sufficiently obvious as to require no further comment.

Utilization of this analysis, however, requires a sensitive, accurate means of monitoring the concentration of $\langle H^{+} \rangle$ (H interstitials) in the crystal. Furthermore, the measurement technique must be non-destructive, since the accuracy required demands that successive measurements be performed on the same specimen to eliminate error due to variation in sample purity, which is unavoidable with presently available crystals. Measurement of the IR absorption associated with $\langle H^{+} \rangle$ satisfies all of these requirements.[2] However, utilization of this technique requires rather precise determination

of the "absorption strength" of the $\langle H^+ \rangle$. Theoretical calculations of sufficient accuracy are not feasible, because of the large dielectric constant and strong anisotropy of rutile, uncertainties as to the $\langle H^+ \rangle$ site in the lattice, etc. A previous paper[2] gave an approximate value for the absorption strength, based on changes in mass of a crystal into which H had been diffused, but the value listed was not sufficiently accurate for our purpose. In this paper we present the results of a refinement of this measurement, yielding accurate values of the absorption strength for both $\langle H^+ \rangle$ and $\langle D^+ \rangle$, together with a detailed discussion of techniques developed to overcome the rather severe experimental difficulties inherent in such a measurement. Work is presently in progress to apply these results and the analysis in the preceding paper[1] to a variety of rutile-impurity systems.

II. Description of Experiment

The basic requirement of the experiment is very simple; to determine precisely the concentration of $\langle H^+ \rangle$ required to produce a given IR absorption. Several techniques were considered, including various chemical determinations, mass spectrometer measurements, NMR, and others. For various reasons, it was decided that direct measurement of the mass changes associated with changes of $\langle H^+ \rangle$ concentration were most likely to yield the required accuracy. In practice, it was found that this straightforward approach was inadequate, for reasons discussed below, and it was necessary instead to measure the mass change associated with the replacement of $\langle H^+ \rangle$ in the crystal with $\langle D^+ \rangle$

(or conversely), in such a way that the total concentration of $\langle H^+ \rangle$ plus $\langle D^+ \rangle$ remained essentially constant. Thus, the measurements consisted of weighing a sample, equilibrated at appropriate H_2O partial pressure and temperature, measuring the IR absorption due to the $\langle H^+ \rangle$, then heating the crystal to the same temperature, with the H_2O replaced by D_2O, reweighing the crystal and measuring the IR absorption due to both $\langle D^+ \rangle$ and $\langle H^+ \rangle$. By cycling the crystal several times and checking at various points in the cycle, it was established that the total concentration of $\langle H^+ \rangle$ plus $\langle D^+ \rangle$ was indeed constant (except as noted below), and the absorption strengths of both the $\langle H^+ \rangle$ and $\langle D^+ \rangle$ were readily obtained. A variety of complications arose in the course of the experiment, as discussed below, but the basic experiment consisted of this simple sequence of measurements.

III. Sample Preparations and Heat Treatment

As shown in the preceding paper[1], the $\langle H^+ \rangle$ solubility is strongly dependent on the density of acceptor levels in the crystal, and because of the very small mass changes expected, it was necessary to utilize crystals containing as high a concentration of acceptors as possible. (An alternative approach would be to H-dope without acceptors, allowing the electrons from the H donors to populate the conduction band; however, the conduction electron absorption is much stronger than, and overlaps the $\langle H^+ \rangle$ absorption peak[2], making accurate measurements unfeasible. Fe and Al were chosen as the most appropriate acceptor impurities, since both have fairly high solubility and were known to diffuse quire readily. Nominally pure crystals were doped by diffusion in sealed, evacuated quartz ampoules, using $AlCl_3$ and $FeCl_3$

as the dopants. It was found that most of the dopant (~ 80%) diffused into the rutile, after heating to ~ 1000°C for 10 to 100 hours, depending on sample dimensions, and that reasonable good control of acceptor concentration could be obtained by careful weighing of the dopant. The solubility of Fe was found to be somewhat higher than that of Al. Not surprisingly, in the light of the discussions in Ref. 1, both were found to depend strongly on μ_e (and hence, on the atmosphere and temperature of heat treatment). In an atmosphere consisting of 22 Torr H_2O and 100 Torr O_2, at ~ 800°C, the Fe solubility was estimated to be ~ $6 \times 10^{19}/cm^3$, and Al solubility was somewhat smaller. When the H_2O was removed from the atmosphere (for example, by use of a liquid nitrogen trap), the solubility decreased dramatically in both cases, resulting in diffusion of the Fe or Al to the surface of the crystal and formation of visible precipitates inside the crystal. Since formation of these precipitates involved a change in the effective valence state of the dopants (presumably both ended up in +3 states, while they had previously occupied lattice sites with an "effective" valence of +4), this process was accompanied by loss of oxygen from the crystal and a corresponding mass decrease, much larger than the expected change associated with $\langle H^+ \rangle$ loss. While this process has not been studied in detail, it is clear that the solubility of acceptor impurities depends strongly on μ_e and that it is not possible to maintain a high concentration in the absence of donor impurities. Thus, it was not possible to perform the desired measurements with sufficient accuracy simply by diffusion of H in and out as originally intended. To circumvent this problem, it was necessary to perform the experiment in such a way as to always maintain a constant (equilibrium) concentration of $\langle H^+ \rangle$ or an entity chemically equivalent to $\langle H^+ \rangle$, i.e., $\langle D^+ \rangle$.

A further complication in such an experiment is that the concentration of donor impurities or defects other than $\langle H^+ \rangle$ or $\langle D^+ \rangle$ must be kept constant and at a very low level. Introduction of donor impurities can be effectively eliminated by careful attention to possible sources of contamination and by maintaining strongly oxidizing conditions during heat treatment. (Hydrocarbons from vacuum pump oil, O-rings, etc., are a major source of contamination; an oxidizing atmosphere renders these innocuous). All heat treatments were performed in clean Vycor tubes, in atmospheres of O_2 and either H_2O or D_2O, and we found no evidence of contamination, even after as many as 20 runs on individual specimens. The problem of lattice defects is more complicated. Since the introduction or removal of $\langle Ti^{+4} \rangle$ (or O-vacancies) again involves large changes in mass, it was essential that these defects either be eliminated or at least maintained at a constant level. After initial doping with Fe or Al, the concentration of defects was quite high. (We assume that the defects are predominantly $\langle Ti^{4+} \rangle$ or possible complexes of interstitials, as mentioned in Ref. 1. However, nothing in our experiment would distinguish between these defects and O-vacancies and none of our conclusions would be changed if O-vacancies were involved.) This high initial concentration of defects was reduced below measurable levels by prolonged treatment in an $H_2O + O_2$ atmosphere at temperatures of 800°C or more, as discussed below. This treatment was accompanied by a mass increase appropriate to removal of a concentration of $\langle Ti^{4+} \rangle$ corresponding roughly to that required to compensate the acceptor impurities which had been introduced; an appropriate simultaneous increase in $\langle H^+ \rangle$ concentration was also observed by IR absorption.

Disc shaped samples 8 to 20 mm diameter and 2 to 10 mm thick, oriented with the flat surface $\perp$ to the c-axis (to eliminate problems associated

with the dichroism of the $<H^+>$ or $<D^+>$ optical absorption[2]) were used, the dimensions being chosen to optimize the sensitivity of the various measurements and to provide reasonable diffusion times at the temperatures used. After Fe or Al diffusion and the H_2O pretreatment outlined above, the crystals were carefully polished on all surfaces. This step is particularly important, since a rough surface is very susceptible to chipping on a microscopic scale, and is difficult to keep clean. The samples were checked for homogeneity by measuring the $<H^+>$ - $<D^+>$ concentration in various parts of the sample. The Al doped crystals were found to be rather inhomogeneous; the Al concentration appeared to be as much as 25% higher near the edges of the crystal than at the center. No significant inhomogeneities were found in the Fe doped crystals; $<H^+>$ concentration was constant to within 2% throughout the crystal. For this reason, and because of the higher solubility, most of the measurements were made on Fe doped material; results on Al-doped crystals were consistent with those for Fe-doped crystals within experimental error.

IV. Optical Absorption Measurements

IR absorption measurements were made on a Beckman IR-12. The peak optical density of the $<H^+>$ or $<D^+>$ absorption line was generally too high for direct measurement (due to the limitations imposed by the sensitivity of the mass measurements discussed below), so measurements were made at various fixed wavelengths on the "tails" of the absorption lines, and the total absorption strength (i.e., the area under the absorption peak) was inferred from this by careful comparison of absorption at these wave-

lengths with the total absorption in thin slices of the crystal. It was necessary to do this separately for each specimen, since the line shape and background absorption varied somewhat from sample to sample, and was, of course, quite different for Fe and Al doped samples.[2] Various checks indicated that these determinations were reliable to ~ ± 2%.

Since the $\langle H^+ \rangle$ and $\langle D^+ \rangle$ absorption line positions and line widths are quite sensitive to temperature, it was necessary to utilize a controlled-temperature sample holder. All measurements reported herein were taken at 35°C.

V. Mass Measurements

The crystals were weighed on a modified Mettler M-5 microbalance. Optimum sample size was in the range from 5 to 20 grams (the maximum capacity of the balance) and the corresponding mass changes expected were ~ 70-300 μ-grams for crystals with maximum Fe concentration. After considerable effort, we were able to obtain sensitivity and reproducibility of better than ± 2μg on a 5g sample, which, with adequate statistics, should permit an overall accuracy of 1 or 2%, which was the goal of the experiment. The absolute accuracy of the mass determinations was substantially poorer, of course, but was of no particular importance in this experiment.

To achieve this degree of reproducibility, rather elaborate precautions were necessary. As previously mentioned, careful polishing of the crystals was essential and extreme caution in handling was still necessary. Plastic tipped forceps were used to avoid chipping and scratching, and sliding the crystal against the walls of the Vycor heat-treating tube was carefully avoided. Ordinary cleaning techniques proved to be adequate,

provided all lint and dust was subsequently removed with an antistatic brush. Adsorption of moisture, etc., on the surface of the crystal was also minimized by the careful polishing and was found not to be a problem.

Appropriate measures were taken to isolate the microbalance from vibration and it was located in a room chosen to minimize temperature fluctuations (the temperature was stable to ± 1/2°C, with negligible short term fluctuations). Nevertheless, temperature stability of the balance was still a major problem. The balance was heavily insulated and the front panel was carefully maintained at a temperature ~ 1°C above ambient by heating elements cemented to the panel. The heating elements were turned off while the balance was in use; this procedure compensated for the temperature rise which otherwise would have resulted from the proximity of the operator. It was also found to be necessary to provide forced-air cooling for the light used to illuminate the balance scale. Remote handling of the samples inside the balance chamber was provided. Introduction of samples into the balance chamber produced fluctuations requiring an equilibration time of ~ 1/2 hour. Appropriate corrections to compensate for variations in atmosphere density were necessary, since the density of TiO_2 is significantly less than that of the balance weights. With these precautions, the measured masses of both the rutile specimens and stainless steel standards were reproducible to ± 3 μg for single readings and significantly better if several readings were taken.

VI. Results and Discussion

A large number of measurements were made on a variety of crystals

(primarily Fe-doped, as discussed previously) and under differing equilibration conditions. The data reported here are for crystals equilibrated at 800°C, in ~ 300 Torr O_2 and 1500 Torr H_2O or D_2O. The exact O_2 pressure could not be determined, but was the same from run to run to within 5%. The crystals were placed in Vycor capsules with ~ 0.1 cm^3 H_2O or D_2O which was then frozen. Next the capsules were evacuated, flushed and filled with O_2 to a pressure of 100 Torr, at which point the capsules were sealed. The capsule was then placed in a 2-zone furnace, with the end containing the crystal maintained at 800°C and the opposite end at 120°C, resulting in the partial pressures indicated above. At O_2 pressures significantly below this value, we observed mass changes as a function of O_2 pressure which indicated a changing and non-negligible concentration of $\langle Ti^{4+} \rangle$. Data taken in this range and at different temperatures can be used to obtain the solubility parameters for $\langle Ti^{4+} \rangle$ and will be reported in a future publication, but for present purposes it is significant to note that data obtained at O_2 and H_2O pressures below 300 and 1500 Torr, respectively, are consistent with the results reported here only if $\langle Ti^{4+} \rangle$ concentration is taken into account in calculating both the mass changes and the donor density. At the pressures and temperature indicated above, our data show that the Ti interstitial concentration is below detectable limits ($2.5 \times 10^{16}/cm^3$). If the $\langle Ti^{4+} \rangle$ concentration is below detectable limits, small unavoidable changes in partial pressures and temperatures produce minor changes in $\langle H^+ \rangle$ and $\langle D^+ \rangle$ concentration, which is properly accounted for by our analysis, but no detectable mass changes due to changing $\langle Ti^{4+} \rangle$ concentration; hence, these data are far more accurate than would be possible in the presence of significant $\langle Ti^{4+} \rangle$. Thus, only a few runs were required to obtain sufficient accuracy after the appropriate operating conditions were determined. Since our main concern here is with the "absorption

strength" of $\langle H^+ \rangle$ and $\langle D^+ \rangle$, we report only data for crystals with negligible $\langle Ti^{4+} \rangle$. All of our data (> 100 runs), however, are consistent with that reported here, if defect concentration is properly taken into account.

The (visible) optical absorption spectrum of these samples is consistent with a charge state of 3+ for the Fe ^{2}. Furthermore, the pressures and temperature above apparently result in a Fermi level significantly above the Fe^{3+} trapping level (but below the Fe^{2+} level), since the $\langle H^+ \rangle$ concentration depends only very weakly on P_{H_2O} (see Ref. 1). Thus, since the Fe concentration is much higher than that of the accidental impurities, and presumably there are no other donors present in significant concentrations, the $\langle H^+ \rangle$ and/or $\langle D^+ \rangle$ concentration should be approximately equal to the Fe concentration. Repeated cycling between approximately 95% $\langle D^+ \rangle$, 5% $\langle H^+ \rangle$ and 5% $\langle D^+ \rangle$, 95% $\langle H^+ \rangle$ (monitored by IR absorption), during which time the total $\langle H^+ \rangle + \langle D^+ \rangle$ concentration remained constant with experimental error (± 2%), indicated a total $\langle H^+ \rangle + \langle D^+ \rangle$ (and hence, Fe) concentration of $5.6 \times 10^{19}/cm^3$.

Since the IR absorption peak shape varies considerably, depending on purity, temperature, etc., we have analyzed our data in terms of the integrated absorption (although, except for calibration, actual measurements were made only at fixed wavelengths, as discussed in Sec. IV), which should be essentially independent of line shape and hence can be used as a measure of $\langle H^+ \rangle$ or $\langle D^+ \rangle$ concentration in any rutile crystal, independent of purity. Let $D_H(\nu)$ be the optical density due to $\langle H^+ \rangle$ in a particular specimen at wavenumber ν and let A_H be the corresponding integrated absorption, i.e.,

$$A_H = \int D_H(\nu) d\nu \qquad (1)$$

$D(\nu)$ is related to the absorption coefficient $\alpha(\nu)$ by the relation

$$D(\nu) = \alpha(\nu)t/2.3$$

where t is the sample thickness in cm. Also, we define a quantity A_H (the "absorption strength" per ion), which we later relate to the oscillator strength, as

$$a_H = \frac{A_H}{n_H t} = \frac{1}{2.3 n_H} \int \alpha(\nu)d\nu \qquad (2)$$

where n_H is the $<H^+>$ concentration in cm^{-3} (note that this is not the same notation used in Ref. 1). Further, we let m_H be the mass of a proton, M_H the total mass of $<H^+>$ in the crystal and M the total mass of the crystal. Then

$$M_H = n_H m_H V = \frac{n_H m_H M}{\rho} \qquad (3)$$

where V is the sample volume and $\rho = 4.26$ gms/cm^3 is the density of rutile. Combining Eq. (1) - (3), and equivalent equations and definitions for $<D^+>$, and letting Δ denote changes in these quantities between successive runs, we obtain

$$\Delta M = \Delta M_H + \Delta M_D = \frac{M}{\rho}(\Delta n_H m_H + \Delta n_D m_D)$$

$$= \frac{M}{\rho}\left(\frac{\Delta A_H m_H}{a_H t} + \frac{\Delta A_D m_D}{a_D t}\right) = \frac{1}{a_H}\left(\frac{M m_H}{t\rho}\right)\left(\Delta A_H + \left[\frac{m_D}{m_H}\frac{a_H}{a_D}\right]\Delta A_D\right) \qquad (4)$$

$$= \frac{K}{a_H}(\Delta A_H + \beta \Delta A_D) \quad ,$$

assuming that all mass change was due only to $<H^+>$ and $<D^+>$, as was the case for our measurements. K contains only known constants and geometrical

factors; the constant β (which would equal 2 if the absorption strengths of $\langle H^+ \rangle$ and $\langle D^+ \rangle$ were equal) can be determined independently of the mass measurements if chemical equilibrium is maintained, since the total concentration of $\langle H^+ \rangle + \langle D^+ \rangle$ will remain constant. (In principle, some departure from this condition might be expected, since the diffusion coefficients for $\langle H^+ \rangle$ and $\langle D^+ \rangle$ should differ slightly, but in practice, this difference was not observed, presumably because changes in chemical potential which would result from changing concentration constitute a much stronger driving force for diffusion than a concentration gradient alone, as discussed later in this section). We evaluated β from absorption measurements taken when the crystal contained (essentially) 100% $\langle H^+ \rangle$, and 100% $\langle D^+ \rangle$, resulting in a value for β of 3.78. The total $\langle H^+ \rangle + \langle D^+ \rangle$ concentration as determined in this way remained constant to within ± 2% over the entire range of $\langle H^+ \rangle / \langle D^+ \rangle$ concentrations. Small variations were to be expected due to the uncertainties in partial pressures; hence, we feel the value of β is accurate to better than ± 2%. Assuming that the uncertainty in the determination of β was smaller than the uncertainty in the determination of a_H, a_H was then evaluated from a least-squares fit of a series of 6 successive runs, yielding a value of $(3.14 \pm .11) \times 10^{17}$, where the error bars represent 90% confidence limits.

To obtain an approximate value of the oscillator strength, f, we applied the Smakula equation[3], in the form

$$f_{H(D)} = \frac{2.3 A_{H(D)} \mu_{H(D)} c^2}{\pi e^2 \, t \, n_{H(D)}} \quad \frac{9n}{(n^2 + 2)^2}$$

where e is the electron charge in esu, n is the refractive index at the stretch frequency, c is the velocity of light, $\mu_{H(D)}$ is the reduced mass of

the oscillator and $\frac{2.3\ A_{H(D)}}{t}$ is the area under the absorption coefficient peak in cm^{-2}. Using the reduced mass of free OH and OD molecules, and a value of the refractive index n = 2.5 (which is the average for the two polarizations), results in identical values for f_H and f_D of 4.66×10^{-2}. This may be compared with values obtained for K and Rb halides of $f_H \sim 5 \times 10^{-3}$ and N_a halides of $\sim 5 \times 10^{-4}$.[3] Thus, the oscillator strength in rutile is considerably larger than that in the alkali halides and that calculated for the free OH^- ion.[4] However, the stretch frequency is significantly shifted to lower energies in rutile, so one might expect a considerable host dependent shift in f also. The exact agreement of f_H and f_D is probably accidental. It should be noted that the values of a_H and β are undoubtedly more accurate than those for f_H and f_D, due to ambiguity of the meaning of $\mu_{H(D)}$ and uncertainty in the appropriate value of n, as well as approximations inherent in the theory. Thus, the quoted values of a_H and β should be used in experimental determination of n_H and n_D.

As indicated in a previous publication[2], the $\langle H^+ \rangle$ line shape in rutile is rather complex and depends on other impurities. The measured peak width at half maximum for the Fe-doped crystals used here was ~ 27 cm^{-1} for the $\langle H^+ \rangle$ absorption at 35°C, which was somewhat larger than for undoped crystals.[2] Comparison of the measured integrated absorption for these crystals with that for a Lorentzian line of the same width and height results in a measured area 10% larger than for the corresponding Lorentzian peak.

In addition to $\langle H^+ \rangle$-associated absorption peaks previously reported[2] at ~ 3650 and 4350 cm^{-1}, we have also observed an absorption peak at 2119 cm^{-1}, the amplitude of which is proportional to $\langle H^+ \rangle$ concentration and is smaller

than the main <H^+> peak at 3279 cm^{-1} by ~ 200X. <D^+>-associated absorption spectra centered at ~ 2800 cm^{-1} (very broad) and 3200 cm^{-1} were also observed. (The latter is difficult to observe, since it is "buried" under the <H^+> absorption). These spectra apparently correspond to the 4350 and 3650 cm^{-1} <H^+> spectra, and have similar absorption strengths. The 4350 cm^{-1} absorption was previously tentatively identified as the 1st harmonic of the 3279 cm^{-1} <H^+> peak. It now appears that this is incorrect, since the ratio of 4350:3279 is almost identical to 3200:2438, which would be very improbable for such strongly shifted harmonic absorptions. Thus, a combination mode absorption for all four of the higher energy satellite absorptions appears to be the most reasonable explanation. This would yield an approximate excitation energy for one of the transverse <H^+> modes corresponding to 4350-3279 = 1071 cm^{-1}. This is slightly more than 1/2 the energy of the 2119 cm^{-1} absorption, which thus could be the 1st harmonic of this transverse mode. Unfortunately, the predicted fundamental at ~ 1071 cm^{-1} falls in the region of strong lattice absorption and is probably not observable. Polarization and temperature dependence studies of these spectra are planned.

It is worth noting that the <H^+>-<D^+> substitution technique described above provides an excellent (perhaps the only) means of obtaining accurate measurements of <H^+> diffusion in such a crystal. Previous attempts have been made to measure <H^+> diffusion[5], but agreement among these measurements has been quite poor. It now seems clear that the difficulties with these experiments stem from two related sources: first, the driving force for diffusion is actually the gradient in the chemical potential; only in

special cases can this be adequately approximated by the concentration gradient, as is usually assumed. In materials like rutile, in which the chemical potential depends strongly on μ_e, which in turn depends strongly on the concentration of $\langle H^+ \rangle$, this may be a very bad approximation. Secondly, as we have shown[1], heat treatment in an atmosphere of H_2, which has been used in most experiments, results in introduction of Ti interstitials, which can seriously affect the results of the measurements in a variety of ways. While the binding energies required for detailed calculations are not yet available, it is clear from the analysis of Ref. 1, that heating in H_2 with no H_2O present, should result in a very high concentration of $\langle Ti^{4+} \rangle$ (see Eq. (22), Ref. 1). We have verified this experimentally by heating an undoped crystal to 800°C in 10 Torr of very dry H_2. This resulted in a substantial concentration of donor interstitials, as indicated by the optical absorption and electronic conductivity ($\sim 10^{-4}/\Omega$ cm), but essentially no H in the crystal ($< 10^{17}/cm^3$, as measured by IR absorption.) This is in marked contrast to the results obtained from heating similar crystals in an atmosphere of H_2O and O_2, which produces large concentrations of H interstitials and, under proper conditions, virtually eliminate Ti interstitials, as discussed above. The technique of $\langle H^+ \rangle$ - $\langle D^+ \rangle$ substitution described above eliminates both of these problems, since chemical equilibrium is maintained at all times. Actually, this is not strictly correct, since the diffusion coefficients for $\langle H^+ \rangle$ and $\langle D^+ \rangle$ should not be exactly the same; our experimental data, however, indicates negligible change in the $\langle H^+ \rangle + \langle D^+ \rangle$ concentration. This observation clearly demonstrates the importance of contributions to the driving force for diffusion other than concentration gradients, since expected departures from chemical equilibrium due to differences in diffusion coefficients are not observed. Thus, the electric fields produced by small

changes in μ_e enhance $\langle D^+ \rangle$ diffusion and retard $\langle H^+ \rangle$ diffusion, so that only the average of the two diffusion coefficients can be observed. Diffusion measurements using this technique are in progress and will be reported in a future publication.

The authors wish to thank Drs. John Shaner and Fritz Lüty for numerous helpful discussions.

REFERENCES

1. John DeFord and O. W. Johnson, preceding paper.

2. O. W. Johnson, W. D. Ohlsen and Paul I. Kingsbury, Jr., Phys. Rev. 175, 1102 (1968).

3. B. Wedding and M. V. Klein, Phys. Rev. 177, 1274 (1969).

4. P. E. Cade, J. Chem. Phys. 47, 2390 (1967).

5. G. J. Hill, Brit. J. Appl. Phys. 1, 244 (1968), and unpublished results by the present authors.

Preprint No. 3

THE BAND GAP ABSORPTION OF RUTILE (TiO_2)*

John W. Shaner
Department of Physics
University of Utah
Salt Lake City, Utah 84112

The existing optical and phonon data on rutile have been examined to determine the band gap of rutile (TiO_2). Arguments are presented for the conclusion that the band gap is indirect, involving electronic transitions between Γ and M or Z and A, and that the gap energy is 3.02 eV.

Any attempt to calculate the band structure of rutile (TiO_2) has in the past been met with a large number of conflicting statements concerning the gap energies. Early optical absorption measurements showed the onset of Urbach tail absorption starting near 3 eV[1], and this has been taken as the gap energy by many authors. Subsequent reflectivity measurements have shown that a significant increase in the absorption coefficient begins to appear only at energies greater than 3.5 eV[2]. Interband Faraday rotation and two photon absorption measurements have led to suggestions of an indirect gap of 3.0 eV with a direct gap of 3.3 eV[3] and a direct gap at Γ of 3.75 eV[4], respectively.

Electromodulation spectra have been measured for rutile[5,6] with the conclusion that there is optical absorption structure around 3.05 eV which is consistent with phonon assisted transitions. From the energy difference between the phonon absorption and phonon emission peaks, an estimate can be made of the phonon energies involved: 30 meV for light polarized $E \perp$ c-axis, and 40 meV for light polarized $E \| $c-axis[5]. Since the energy halfway between the phonon emission and phonon absorption peaks is the same for both polarizations, we may assume, as in Ref. 5, that the initial electronic states are the same, and final electronic states are the same, for both polarizations.

Recent neutron scattering experiments, elucidating the phonon structure[7], allow one to fit the electromodulation data and to establish the possible initial and final electronic states. Since both the initial states and the final states are the same for both polarizations, then by k-vector conservation the phonons must come from the same point of the Brillouin zone. From the measured phonon dispersion curves[7], only one such point, the M point (zone boundary in the [110] direction --

has a significant phonon density of states. At the M point, there are two phonon modes with the symmetry[8] M_5 or M_6 degenerate at 39 meV and a phonon mode with M_9^+ symmetry at 32 meV. These energies agree with the electro-absorption results to within the quoted experimental uncertainty. We may, therefore, assume that the indirect transition near 3.05 eV involves an emitted M point phonon and an energy gap between electronic states of 3.02 eV. K-vector conservation restricts the electronic transitions involving initial and final states at high symmetry points to 1) $\Gamma \rightarrow M$, 2) $M \rightarrow \Gamma$, 3) $X \rightarrow X$, 4) $Z \rightarrow A$, 5) $A \rightarrow Z$, and 6) $R \rightarrow R$.

The number of possible assignments may be significantly reduced by calculating the allowed phonon assisted transitions between the various electronic states. The correct assignment must involve an M_5 or M_6 phonon for the $E||c$ polarization and an M_9^+ phonon for the $E \perp c$ polarization, and it must have the same initial electron state and the same final electron state for both polarizations. Following the selection rule calculating procedure of Lax and Hopfield[9], and the character tables of Gay, et al.[8], we have calculated the selection rules which satisfy these criteria[10]. The $X \rightarrow X$ transitions and the $R \rightarrow R$ transitions can easily be eliminated. The allowed indirect $X_i \rightarrow X_i$ transitions involving the appropriate phonon symmetries and light polarizations are $X_1 \rightarrow X_1$ and $X_2 \rightarrow X_2$. Since both of these are also allowed direct transitions for $\hat{X}$ polarized light, one would expect a strong zero phonon absorption in addition to the phonon-assisted transitions. Since this behavior is not observed, the pertinent electron states are not at X. The allowed $R \rightarrow R$ indirect transitions would not be allowed direct transitions, but the M_9^+ phonon assisted transition would be allowed for both polarizations for given initial and final states.

Thus, the polarization dependence of the electromodulation data rules out R → R transitions. The remaining allowed transitions subject to our restrictions are presented in Table I. If one assumes that the valence bands are made up of O^{2-} 2p states and the conduction bands are made up of Ti^{4+} 3d states, the allowed initial and final states are further restricted to those bands made up from these atomic states. In particular, this selection eliminates Γ_5^+, Γ_1^-, Γ_2^-, Γ_3^-, and Γ_4^- as possible final states and Γ_2^- and Γ_3^- as possible initial states[11].

A suggestion has been made that the highest valence band and the lowest conduction band at Γ have Γ_3^+ symmetry[4]. If it is assumed in addition that, as in $SrTiO_3$[12], the highest valence and lowest conduction states at the high symmetry points are on the same sheets as those at Γ, then the compatibility relations require the M states to have M_3, M_4, or M_9^+ symmetry, and the Z states to have Z_3 symmetry. From Table I, it is clear that in this case the 3.02 eV electronic transition would be $\Gamma_3^+ \rightarrow M_{3,4}$, $M_{3,4} \rightarrow \Gamma_3^+$, $Z_3 \rightarrow A_{2,4}$, or $A_{2,4} \rightarrow Z_3$.

Apart from the symmetries involved in the indirect transition, there is still a question of excitonic structure. Since the selection rules for transitions to an S-exciton are the same as those to the continuum, one might expect to see transitions to a bound excitonic state as much as several tenths of an eV below the continuum. In fact, additional structure in the electromodulation spectra is observed at 3.10 eV[5] and at 3.3 eV[6]. If the 3.02 eV electronic transition were to an S-excitonic state, and one of the higher transitions were to the continuum, the same polarization dependence of the energies should be observed for both transitions. The 3.10 eV transition energy is independent of polarization, and the 3.3 eV transition is clearly observed only for the E|| c-axis polarization. Since

neither of these polarization dependences is expected if these transitions are to continuum states above a bound exciton at 3.02 eV, we conclude that there is no evidence for bound excitons.

These considerations lead to the conclusion that the structure observed near 3.05 eV in electromodulation spectra of rutile arises from an indirect electronic transition between Γ and M or Z and A, with phonon emission. The energy difference between electronic states is near 3.02 eV. This conclusion is consistent with electromodulation[5,6], interband Faraday rotation[3], and band edge optical absorption[1] data. Since the electromodulation data is obtained optically from an intrinsic crystal, the renormalization of conduction electron energy due to polaron effects should not contribute to the 3.02 eV energy gap. This gap will then be appropriate for the rigid ion band calculations. Such detailed symmetry information for interband transitions in rutile has not previously been available. We suggest that it should be useful as a constraint on any band structure calculation for rutile.

REFERENCES

1. D. C. Cronemeyer, Phys. Rev. 87, 876 (1952).
2. M. Cardona and G. Harbeke, Phys. Rev. 137, A1467 (1965).
3. W. S. Baer, J. Phys. Chem. Sol. 28, 677 (1967).
4. H. S. Waff and K. J. Park, Phys. Lett. 32A, 109 (1970).
5. F. Arntz and Y. Yacoby, Phys. Rev. Lett. 17, 857 (1966).
6. A. Frova, P. J. Boddy, and Y. S. Chen, Phys. Rev. 157, 700 (1967).
7. J. G. Traylor, et al., Phys. Rev. B3, 3457 (1971).
8. The notation is that of J. G. Gay, W. A. Albers, Jr., and F. J. Arlinghaus, J. Phys. Chem. Sol. 29, 1449 (1968).
9. M. Lax and J. J. Hopfield, Phys. Rev. 124, 115 (1961).
10. A more complete listing of direct and indirect transition selection rules for the rutile group (D_{4h}^{14}) will appear in a more extensive paper.
11. These symmetries are taken from Reference 4. Care should be used in comparing results, however, since the notation of Reference 4 is not the same as that of Reference 8, which is used here.
12. A. H. Kahn and A. J. Leyendecker, Phys. Rev. 135, A1321 (1964).

* This research supported by the Advanced Research Projects Agency on Contract No. DAHC-15-71-G8.

Table I Allowed phonon assisted electronic transitions involving an M_5 or M_6 phonon for $\hat{z}$ polarized light and M_9^+ phonon for $\hat{x}$ polarized light.

Initial (final State	Final (initial) State
Γ_1^+, Γ_4^+	M_1, M_2
Γ_2^+, Γ_3^+	M_3, M_4
Γ_1^-, Γ_4^-	M_5, M_6
Γ_2^-, Γ_3^-	M_7, M_8
Γ_5^+	M_9^+
Z_1, Z_3	A_2, A_4
Z_2, Z_4	A_1, A_3

FIGURE CAPTION

1. Symmetry points of the Brillouin zone for the rutile structure (D_{4h}^{14}).

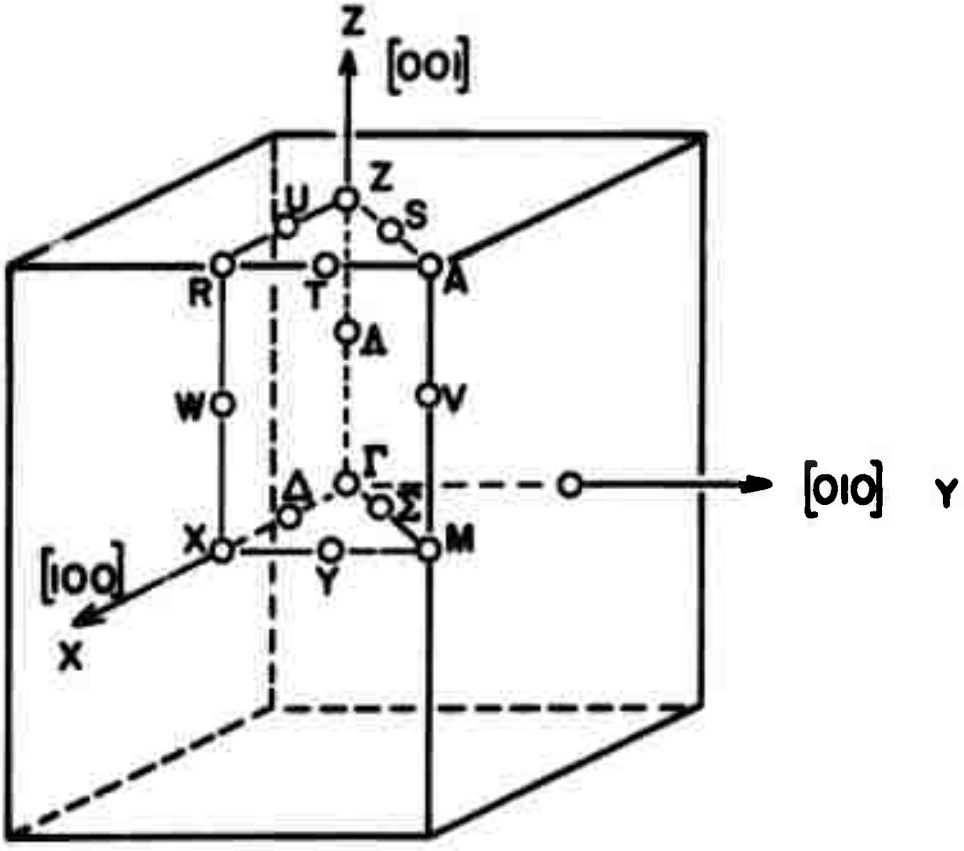

Fig. 1

Preprint No. 4

"Vacuum Reduction" of Rutile*

W. D. Ohlsen and O. W. Johnson
Department of Physics, University of Utah
Salt Lake City, Utah 84112

"Vacuum reduction" of rutile in the temperature range normally employed is shown to be caused by residual vacuum system impurities.

* This research supported by the Advanced Research Projects Agency on Contract No. DAHC-15-71-G8.

The process of heating rutile (TiO_2) in vacuum to achieve non-stoichiometry, and the associated n-type conductivity and blue coloration, has been used by scores of authors in many different investigations[1], and is one of the "standard" experimental techniques in rutile research. It is the purpose of this letter to show that this so-called "vacuum reduction" is in fact a poorly defined and uncontrolled process resulting from contaminants in the vacuum system (i.e., pump oil, water vapor, etc.). As a "dirt" effect, which could involve impurity doping of the crystal, "vacuum reduction" is obviously not a desirable experimental technique. In fact, the term "vacuum reduction" in this context is quite misleading, since the process does not occur in a clean vacuum, and may not even involve "reduction", which implies oxygen-deficient non-stoichiometry. Since the term is in common usage, however, we will continue to use it (with quotation marks), with the understanding that it refers to whatever processes lead to n-type conductivity and blue coloration when rutile is heated in a dirty vacuum, and that it may involve doping with donor impurities rather than true reduction.

Qualitative observations that both the rate and degree of "vacuum reduction" were strongly dependent on the quality of the vacuum system has led many, though by no means all, of those studying this material to the view that "vacuum reduction", at least below 1000°C, is strictly a dirt effect[2]. To the best of our knowledge, however, this assumption has not previously been quantitatively tested. It seemed likely that "vacuum reduction" was not qualitatively different from treatment in an H_2 atmosphere, which is known to involve both H-doping and introduction

of Ti Interstitials[3]. Recent work on Cr^{3+}-associated defects in rutile[4], however, appears to require a qualitative difference between these two processes, and stimulated this more careful investigation of the nature of "vacuum reduction".

The experiment described below was sufficiently clean to establish that most of the reports of "vacuum reduction" have resulted from vacuum system contaminants. A cryscal of nominally pure rutile[5] was first oxidized in pure, very dry oxygen at 800°C. The crystal was then placed in an O-ring-free glass system, consisting of a charcoal trap, 2 ℓ/sec Vacion pump, and fused quartz sample tube. The major aim of the system design was to avoid pump oil contamination. The system was rough-pumped, then sealed, after which the charcoal trap was cooled to 77°K and the rest of the system was baked at 200-300°C for three hours. This modest bake-out was the weakest feature as far as cleanliness is concerned. After bake-out, the Vacion pump and quartz tube were sealed off from the charcoal trap and removed from the bake-out furnace. In less than 1/2 hour the Vacion pump had reduced the system pressure to about 10^{-7} Torr.

The peak optical absorption coefficient at 1.55μ, $\vec{E} \perp$ c-axis, was monitored as a measure of the degree of "reduction". This absorption, resulting in the characteristic blue coloration previously referred to, is due to conduction electrons and is directly related to the number of defects or donors introduced into the crystal[3]. The optical measurements were made through the quartz tube at room temperature without breaking vacuum. Figure 1. shows the peak optical absorption coefficient,

temperature of the sample heating furnace, and vacuum in the sample tube (measured with the Vacion pump) as a function of sample treatment time. The effects of out-gassing of the quartz tube and sample are clearly evident in the vacuum readings and in the slight initial coloration of the sample. The last heat treatment was done in a different furnace which heated a larger portion of the sample tube, resulting in strong outgassing from a portion of the tube not previously heated. The optical absorption coefficient at 1.55μ rose to over $100cm^{-1}$. The increase in pressure precludes the certain identification of the strong coloration at 1150°C as being true vacuum reduction. However, the fact that there was no observable change in sample coloration during 23 hours at over 1000°C clearly demonstrates the absence of true vacuum reduction at this temperature and below. For comparison, a typical treatment which involved heating at 820-850°C for 30 minutes in vacuum of 10^{-2} Torr has been reported[6] to yield an optical absorption coefficient of $13cm^{-1}$.

The nature of neither the slight initial "reduction" nor the strong "reduction" at 1150°C is known at present, although it is clear that at least the initial coloration was due to residual contamination. It was, however, established that neither of the "reduction" processes resulted from H-doping. The H concentration, determined by IR absorption[3] at $3279cm^{-1}$, remained below detectable limits throughout the experiment.

The question of what really happens during so-called "vacuum reduction" is still open. It could be that the "dirt" fills a purely catalytic role producing either Ti interstitials or O vacancies, or that

impurity doping of the crystal takes place. This question is under further investigation.

The nature of the donor defects introduced at 1150°C was examined briefly by ESR. After heating to 1150°C, the sample yielded an intense ESR spectrum at 4°K, similar to that reported by Chester[7] for "vacuum reduced" material. An attempt was made to oxidize the crystal step by step and check the ESR at each stage. Unexpectedly, a 25 hour treatment in 100 Torr of oxygen at the low temperature of 490°C removed practically all (> 90%) of the coloration. The ESR spectrum, however, was practically unchanged. The remaining coloration was quite resistant to oxidation. The oxidation behavior was comparable to that of samples containing Ti interstitials, but no Ti^{3+} ESR spectrum was seen. All of the known dopants which diffuse appreciably at 490°C (Li, H, Na) can be eliminated as the source of the easily oxidized component of the coloration. It would be reasonable to assume that a defect species produced by true vacuum reduction has been observed. It is possible that this defect is involved in Lange's[8] experiment on microwave acoustic relaxation in rutile. Lange obtains "vacuum reduction" in a good (10^{-7} Torr), but perhaps not clean, vacuum at both 850°C and 1050°C, but only observes appreciable acoustic attenuation after the higher temperature treatment.

On the basis of the results reported here and other work on the thermodynamics of H in rutile to be published shortly, it is strongly recommended that "vacuum reduction" be avoided as a technique for inducing n-type conductivity. Departure from stoichiometry can readily be achieved by diffusion of evaporated Ti in a very clean vacuum at temperatures of ~ 800°C. Alternatively, n-type conductivity can be induced by H-doping at lower temperatures.

The thermodynamics of this process, however, is quite complicated, and can, under certain circumstances, result in production of Ti interstitials as well as H interstitials. In most cases, if the doping is carried out in a clean ambient, containing both H_2 and H_2O, only H interstitials result. This problem will be dealt with in detail in a forthcoming publication[9].

The authors acknowledge with pleasure the useful discussions with their colleagues, in particular with Dr. John Shaner.

References

1. This is not the place to list all the implications of this Letter for the conclusions reached in these other investigations. The interested reader is referred to a forthcoming rutile review paper being prepared in this laboratory.
2. H. P. Frederikse: Private Communication
3. O. W. Johnson, W. D. Ohlsen, and Paul I. Kingsbury, Jr., Physical Review 175, 1102, (1968)
4. L. S. Sochave, I. I. Reshina, and D. N. Merlin: Sov. Phys. Solid State 12, 946 (1970). (Fiz. Tver. Tela 12, 1214)
5. The material was nominally pure rutile obtained from the Nakazumi Crystals Corp.
6. V. N. Bogomolov, E. K. Kudinov, D. N. Merlin, and Yu A. Firsov; Sov. Phys. Solid State 9, 1630 (1968). (Fiz. Tver. Tela 9, 2077 (1967))
7. P. F. Chester, J. Appl. Phys. 32, 2233 (1961).
8. James N. Lange, Phys. Rev. 179, 860 (1969).
9. J. W. DeFord and O. W. Johnson, to be published.

Fig. 1. Plot of peak optical absorption coefficient, sample heating furnace temperature and sample tube vacuum vs. sample treatment time. The optical absorption is for light of 1.55μ wavelength with electric vector perpendicular to the c-axis. Each dot corresponds to a measurement. The lines serve only to connect the dots. Vertical segments indicate readings made before and after optical measurements at room temperature.

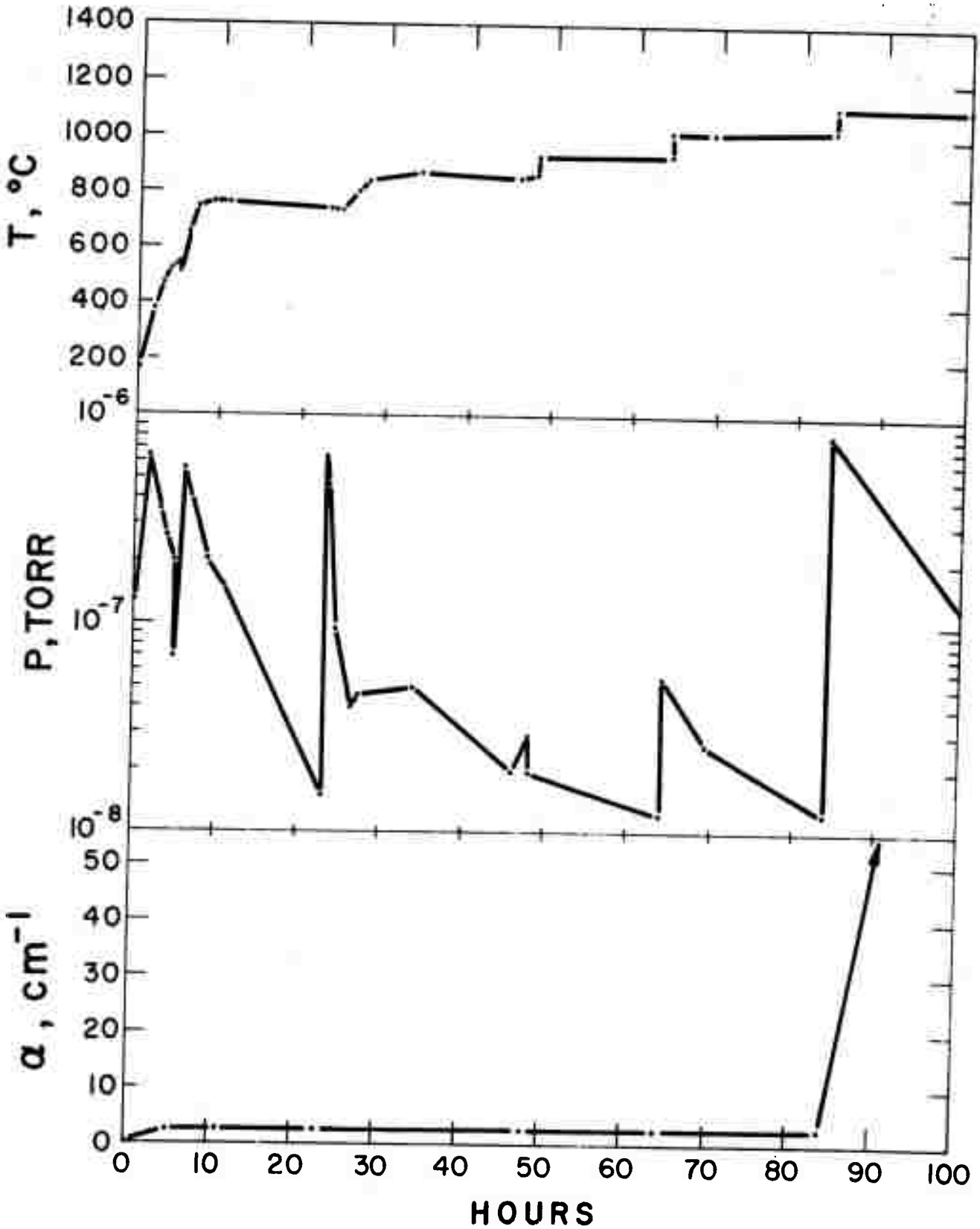
T, °C
1400
1200
1000
800
600
400
200
P, TORR
10^{-6}
10^{-7}
10^{-8}
α, cm^{-1}
50
40
30
20
10
0
0
10
20
30
40
50
60
70
80
90
100
HOURS